STRESS CONCENTRATION IN THE EYE SECTION OF A CONNECTING ROD

BY

BAL D. KALELKAR

B.E., University of Bombay
1940

Submitted in Partial Fulfillment of the
Requirements for the Degree of

MASTER OF SCIENCE
in
MECHANICAL ENGINEERING

from the
MASSACHUSETTS INSTITUTE OF TECHNOLOGY
1941

SIgnature of Author _____
Department of Mechanical Engineering, July 31, 1941

Signature of Professor
in Charge of Research _____

Signature of Chairman of Department
Committee on Graduate Students

Graduate House, M.I.T.
Cambridge, Mass.

July 31, 1941

Prof. G.W.Swett
Secretary of the Faculty
Mass Institute of Technology
Cambridge, Mass.

Dear Sir,

In partial fulfillment of the requirements for the Degree of Master of Science, I hereby submit this thesis entitled, 'STRESS CONCENTRATION IN THE EYE SECTION OF A CONNECTING ROD.'

Respectfully yours

Bal D. Kalelkar

Table of Contents

ACKNOWLEDGEMENT

The author of this thesis would like to express his deep appreciation to Prof. W:M: Murray and Prof. E.S.Taylor for the invaluable assistance and guidance in the work and for suggesting the problem.

The author would also like to take this opportunity of thanking with gratitude Dr. Durelli for his assistance received during the experimental and mathematical work on the subject.

The author is also thankful to Mr. R.A.Frigon for his assistance in photographic work, and Mr. R.P. Misra for his invaluable help in doing the most tedious work of writing the formulas and other eleventh hour work.

XXXXXXXXXXXXXXXX

Purpose of the Investigation

As is known to every engineer, the inertia force produced by the reciprocating piston in an engine, is directly proportional to the square of the speed of the engine, and is maximum at the dead centers, where the piston changes its direction of motion. Due to this force at the top dead center, the connecting rod is subjected to a momentary tensile stress of considerable magnitude. With the development of the high speed engines, the problem of the stress concentration in the eye-section of the connecting rod due to this tensile stress, became more and more important, the increase in the importance being directly proportional to the square of the piston speed.

If the reader traces the motion of the connecting rod of an engine, he will see that the latter is subjected to the following kinds of loading:

Suction Stroke and Compression Stroke

During this stroke, the piston tries to lag behind the piston pin and consequently, the tensile stress is produced in the connecting rod, which is solely responsible for opposing the lagging tendency of the piston. At the end of the suction stroke, due to the inertia of the piston, the piston tries to continue its motion in the

direction of the shaft, while the connecting rod changes its direction, and so a compressive stress is exerted on the connecting rod, during this change of the direction of the piston, and also during the next compression stroke.

Power Stroke and the Exhaust Stroke

Somewhere near the next top dead center position, the explosion takes place, and the piston continues to exert a compressive force on the connecting rod during this power stroke and the next exhaust stroke.

At the end of the exhaust stroke the pressure on the top of the piston being only that of the atmosphere, the inertia force of the piston produces a tension on the connecting rod and hence the latter is subjected to a considerable amount of tensile stress. The present paper is concerned with the investigation of the stress concentration due to this tensile stress.

The author would like to warn, however, that this is not the only critical condition under which a connecting rod is subjected. Due to the sideway motion of the connecting rod, and due to the bending and buckling, the various kinds of complicated stresses are produced in the body of the connecting rod; but as far as the eye-section of the rod is concerned, the tensile stress described above is perhaps the most critical of all.

This leads the designer to the question of investigating the stress concentration in the eye-section of a connecting rod and the author of the present paper has tried to investigate that concentration in an actual connecting rod.

Next the question arises why should one worry so much about this stress concentration when it is possible to increase the thickness of the eye-ring without any appreciable difficulty with regard to the working of the engine? But the problem becomes more important in the design of the connecting rod for an aero engine, where the reduction of even an ounce of metal would be welcomed by the designers and where the use of the high speed engines has become quite common. In the case of the high speed engines the heavy connecting rods would give a headache to the engineers when the latter tries to compensate the out of balance forces of the engine.

All these difficulties make the problem of the stress concentration very important and very interesting.

As the reader would see from the above discussion, the problem of the stress concentration is more important in the case of the aero engines than any other kind. Because of this reason, the author has particularly made his test model of the same type as that used in an aero engine of the radial type. The only change that the author has

made in the model is that the thickness of the eye-section was kept the same as that of the I section of the connecting rod, while in the case of the actual rod, that thickness was 1/16" more on both sides. This change was made on the assumption that it would produce no effect whatsoever on the stress concentration except the increase in stress that would be produced due to the change in the actual cross-sectional area of the eye. The author was convinced about the correctness of this assumption from the results that he obtained during his treatment of the subject, by the three dimensional method.

The writer would like to state here, however, that the work done in this thesis is just one of the series of experiments that the designer must perform to get sufficient data for the connecting rod design. As the reader would see from the discussion on the result of this investigation, one must also find out the stress variations in other cross-sections of the rod, besides the two sections treated in this paper. Again, we must treat the whole problem anew, by changing the inside and outside radii of the eye-section (r_i and r_a), and from all these results, one must find out, a general empirical formula for the design of the eye section. So, the reader would see that the work done here is just a drop in the vast ocean of the data on the connecting rod design.

Previous Work

Before the writer starts giving in detail his method of attack, the results and mathematical calculations, he would like to give in short, the review of the mathematical and experimental work done by the other investigators. The writer would like to divide the articles into three catagories:

a). Experimental investigation,

b). Descriptive treatment,

c). Mathematical treatment.

a). Experimental Investigation: As far as the writer is able to find out, the only photo-elastic analysis that has been done on the subject is by Kango Takemura Kogakuhakusi and Yehei Hosokawas, from the Aeronautical Research Institute, Tokyo Imperial University, in 1928. But as the writer of the present paper has expressed in the above section of this work, done by Kango and his colleague, is also just another drop in the ocean of the knowledge about the stress concentration in the eye section; and though this work is good for guidance, as it is complete in itself. Of course, it is true, that in those days the photoelasticity was not so much developed as it is today and so one cannot expect a better treatment than that we find in this paper.

In their paper the authors give the (p-q) curves

at the critical sections for the four different kinds of eye bars and compares them with the p-q curves obtained for the critical section of a circular ring and an infinite plate with a circular discontinuity. They also give the Isoclinics and the Stress Trajectories for those forms of the eye bars though the author of the present paper has his doubts about the correctness of some of those stress trajectories.

On the whole the article is very good and gives a general idea about the effect of the change of shape on the stress distribution and the stress concentration in an eye bar.

Coming to the second article which appeared in Forschungsarbeiten Heft 306, and which was written by Dr. Mathar, in 1928, the article deals with the results of the experimental determination of the stress variation in the different kinds of eye bars. In his experiments, Dr. Mathat has used the strain method for finding the stresses. He also gives the stress curves for the different sections of the connecting rods. Unfortunately, however, the writer of the present paper cannot read German and so is unable to give a better and more detailed review of Dr. Mathar's work. The results obtained in the present paper tally somewhat with the results of Dr. Mathar. Dr, Mathar's paper seems to be very interesting and important too.

Descriptive Treatment

Coming to the second category the author is able to find only two articles which give in detail the different shapes of the connecting rods.

The article by Mr. Volk in V.D.I.Ziet. Oct.22, 1938, gives in detail the different forms of connecting rods used and proposed for different kinds of engines.

The other article written by Mr. Angle, (Automotive Industries, March 1935) gives much information regarding the ratios of different dimensions of the connecting rods used in present day practice. He also gives a general empirical formula for the design of the eye section but he does not give any proof for the same.

c). Mathematical Treatment

Coming to the mathematical treatment, one article has appeared in "Machine Design" of September 1939. In this article, Mr. K.E.Bisshopp treats the eye section as a curved beam and uses the method suggested by himself in "Machine Design" of August 1937. Mr. Bisshopp gives a series of curves obtained by the mathematical treatment for different ratios of the inside and outside radii of the eye bars. In his article he shows how the stress concentration can be read directly from those curves.

The author first tried to apply this new method of calculations for his model of the connecting rod, but

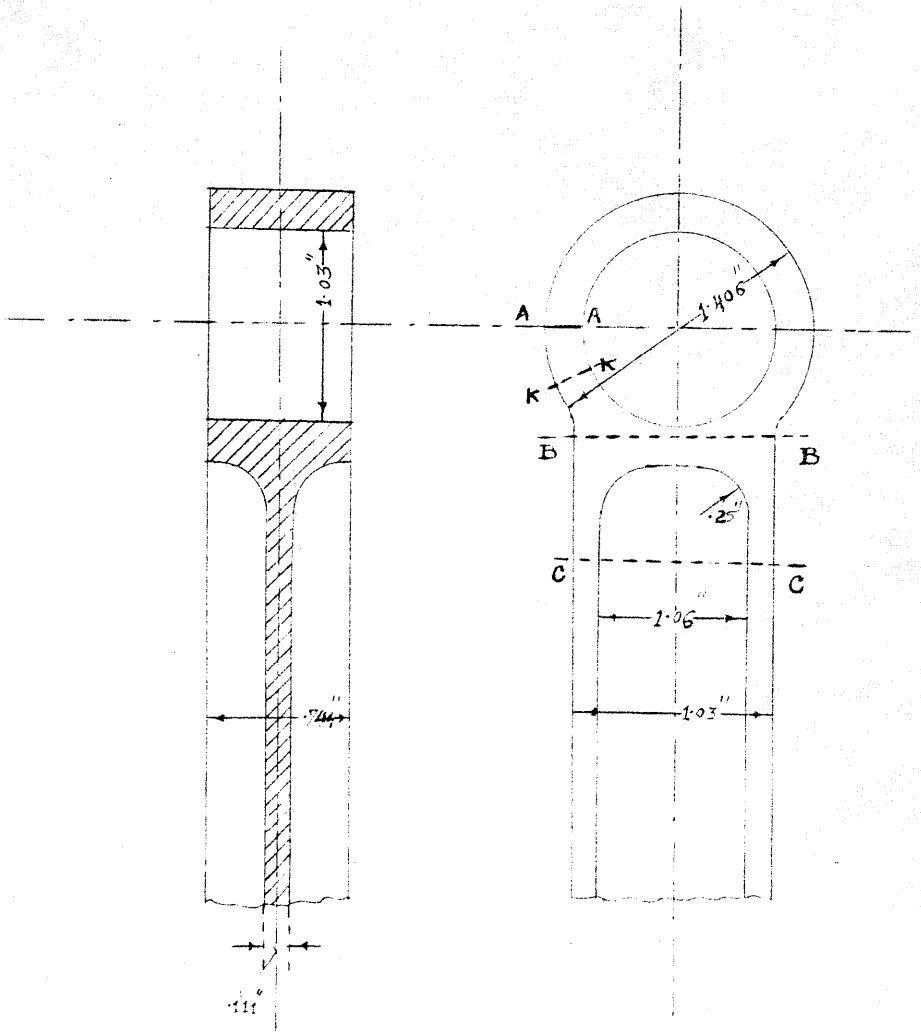

Connecting Rod

Fig. 1

found out at the end that although the method is easier to follow, the results, in case of an actual connecting rod, were quite absurd. The author is of the opinion that the consideration of the eye section as a curved beam is not justified in the cases where the width of the eye ring ($r_a - r_i$) is very small and where the curvature of the section is too great compared to that width. In an actual connecting rod the width is small and the curvature is large.

Coming to the last article by Mr. H.Reissner of Berlin, the article treats the eye section of an connecting rod by the application of the Theory of Elasticity. The article is a thorough treatment on the subject. In his theoretical study the author has been compelled, in common with the other investigators, to make a number of assumptions, not only to simplify the mathematical work but also to make it possible. In his article, Mr. Reissner has treated the problem for four different sets of conditions, i.e., the four different kinds of conditions at the inside and outside edges of the eye ring.

The article is excellent as far as the mathematical treatment of the subject is concerned, and the writer of the present paper has used his method for the calculations of the stresses for his connecting rod. Mr. Reissner, in his paper, calculates the stress varia-

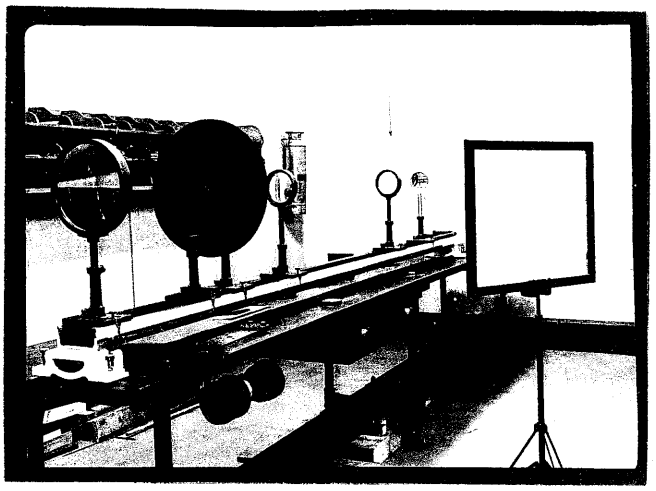

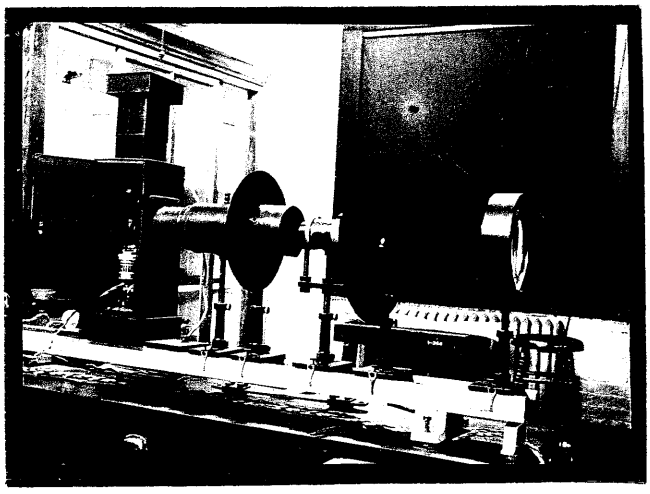

FIG II

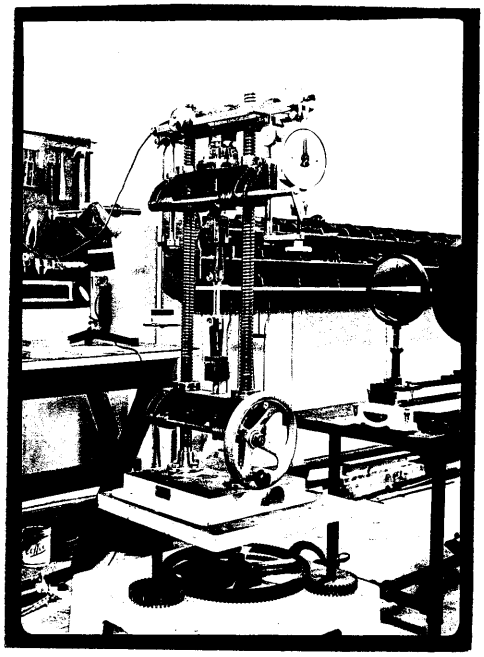

FIG III

tion for two eye bars having the ratios of $\frac{r_a}{r_i}$ = 2 and 4. Though these ratios make the calculations easier to work, the ratios are not used in actual practice and so the work done by Mr. Reissner is useful only for comparison purposes.

As stated above, the author has followed the method given in this article and so the details of the method will be given at a later stage.

The Procedure

A connecting rod was machined from the Bakelite BT 61-893 and the dimensions were made three fourths of the dimensions of an actual connecting rod of a radial aero engine. (Fig. 1). This connecting rod was tested by the two dimensional method as well as by the three dimensional method.

The apparatus used in these experiments were:

(a) A standard type of polariscope which is shown in Fig. 2.

(b) The loading arrangement was also of just the standard type as that shown in Figure 3.

(c). For finding out the values of (p + q), the author used an interferometer strain gage, developed at M.I.T.

All these instruments are of the standard type and so the author does not find it necessary to describe

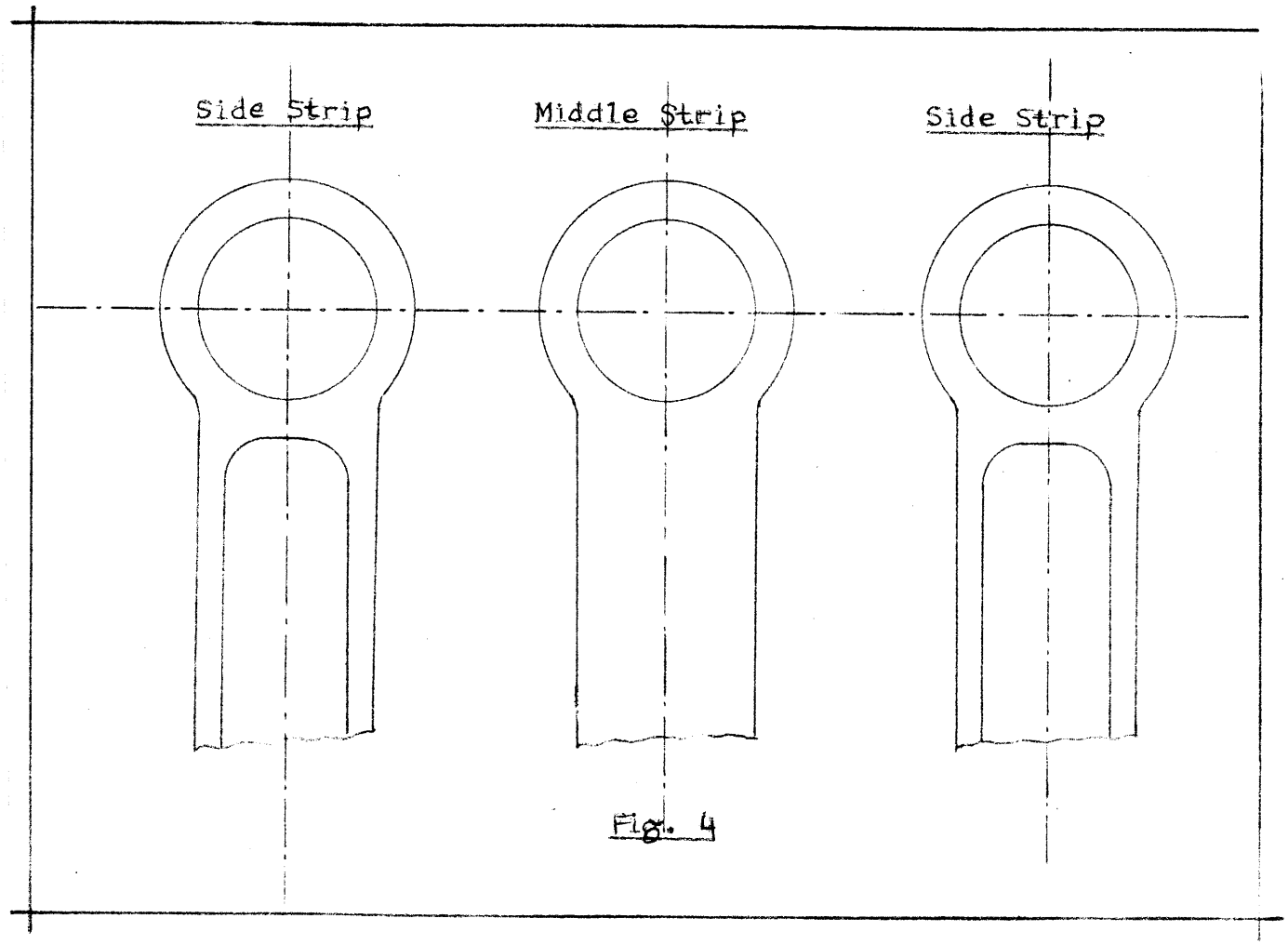

Fig. 4

them in detail and thinks that the photographs given in the Figures 2 and 3 will explain everything, without any difficulty.

The Method of Attack:

In case of a problem in Photoelasticity, the first question that arises is whether the three-dimensional treatment is necessary for the particular problem.

In the present case of the connecting rod, after a thorough study of the case by the three dimensional method, the author of this paper has come to the conclusion that though the problem does appear to be in the three dimensions, the Three Dimensional attack is absolutely unnecessary from the point of view of the stress concentration. The region, at which the effect of the three dimensions takes place, is subjected to such low stress, and the effect of the stresses at this region on the stress concentration in the ring are so negligible, that the three dimensional attack becomes unnecessary.

How Three Dimensional Treatment is Unnecessary

The model of the connecting rod was loaded with a load of 7.5 lbs. (though the author must confess that to keep this load constant was very difficult at high temperatures as the material became plastic and that the author has only tried to keep the load constant, as far

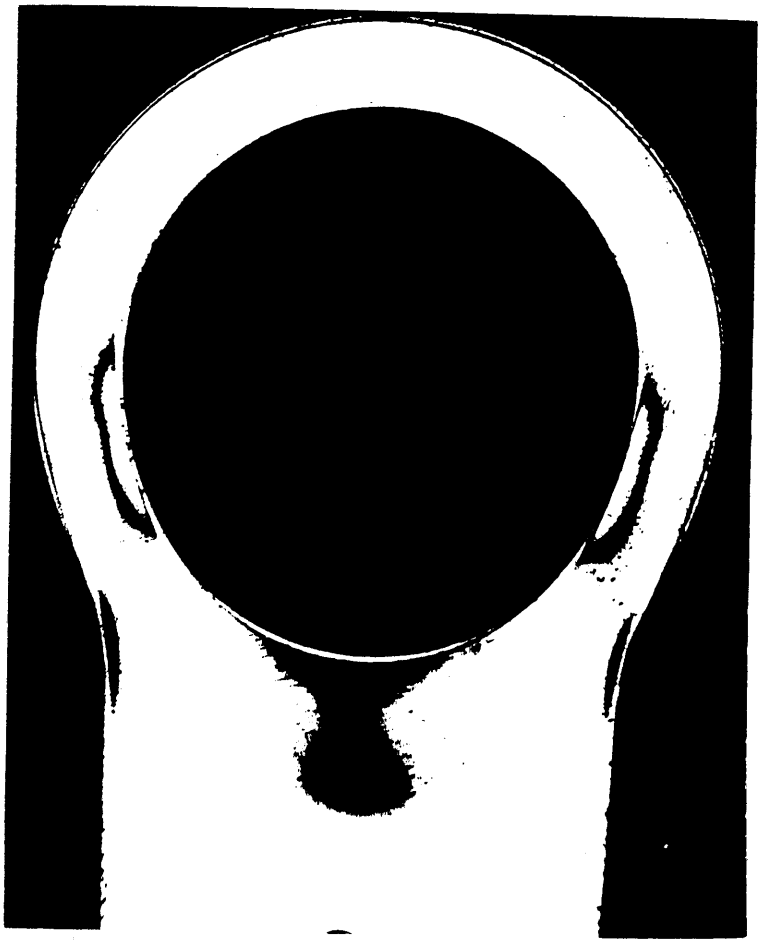

FIG. 5.

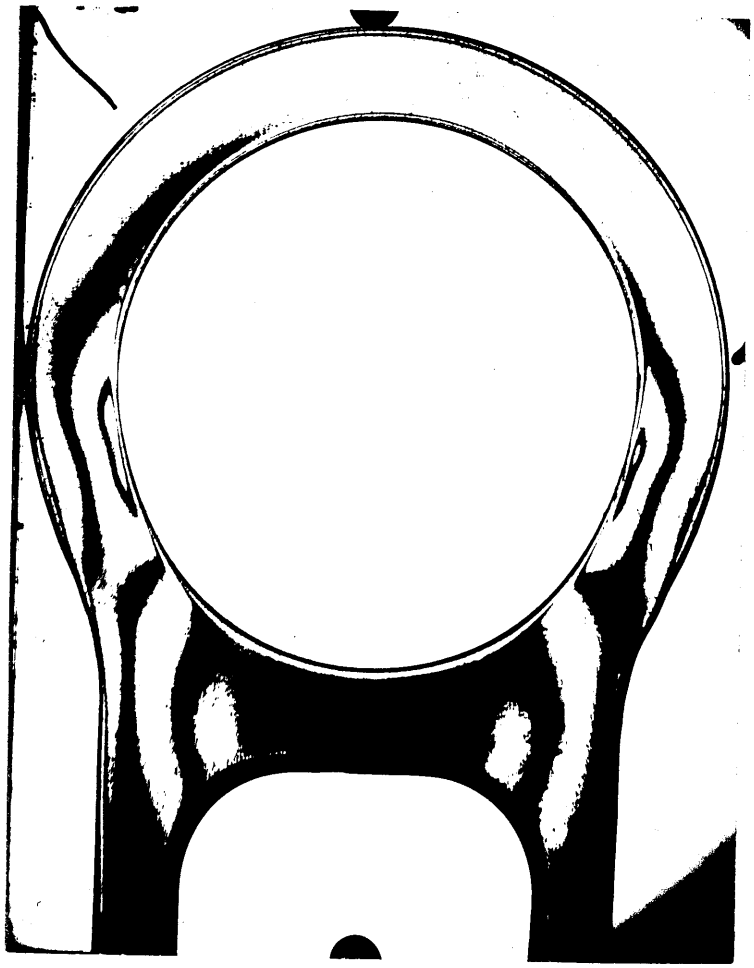

FIG. 6

as was possible.) under a temperature of 115°C. This temperature was obtained gradually within 3 hours. The model was kept at that temperature only for 14 hours. The temperature was then gradually reduced to 70°C in 8 hours. Again this temperature was maintained for the next 14 hours and then the temperature was brought to the normal room temperature in about 6 hours. The model was then cut into three pieces as shown in Figure 4 and the fringe photographs were taken. (Figs. 5 and 6)

Now from these photographs one sees that if one superimposes the fringe photograph of the middle-strip on that of the side-strip, the position of the concentration of the fringe pattern is the same in both the cases. Again, if one calculates the value of (p-q) stresses at these points of the maximum concentrations, one sees that the stresses in both the cases are almost the same. (The reader is warned here not to get misled from the actual photographs, where the number of lines are not the same, due to the fact that the thicknesses of the two strips are not the same.) The calculations for this follow.

The data obtained from the Fringe photographs of the two strips (the middle and the side strips).

The Middle Strip:-

thickness = .087"

maximum fringe order = 1.5

Fringe order in the shank (I section) = .75

The Side Strip:-

Thickness = .165"

Maximum fringe order = 3

Fringe order in the shank (I section) = 1.5

Now say, K is the fringe constant for the material at this elevated temperature; then, maximum value of the (p-q) curve for both the cases will be as follows:

For the middle strip:-

$$(p-q) = \frac{1.5 \times K}{.087} = 17.3\ K$$

For the side strip:-

$$(p-q) = \frac{3 \times K}{.165} = 18.18\ K$$

Again (p-q) = value for the shank (I section) will be

For the middle strip

$$(p-q) = \frac{.75 \times K}{.087} = 8.61\ K$$

For the side strip

$$(p-q) = \frac{1.5}{.165} \times K = 9.09\ K$$

In all the above cases, the value of q is 0; and so the p-q gives directly the stresses at these points.

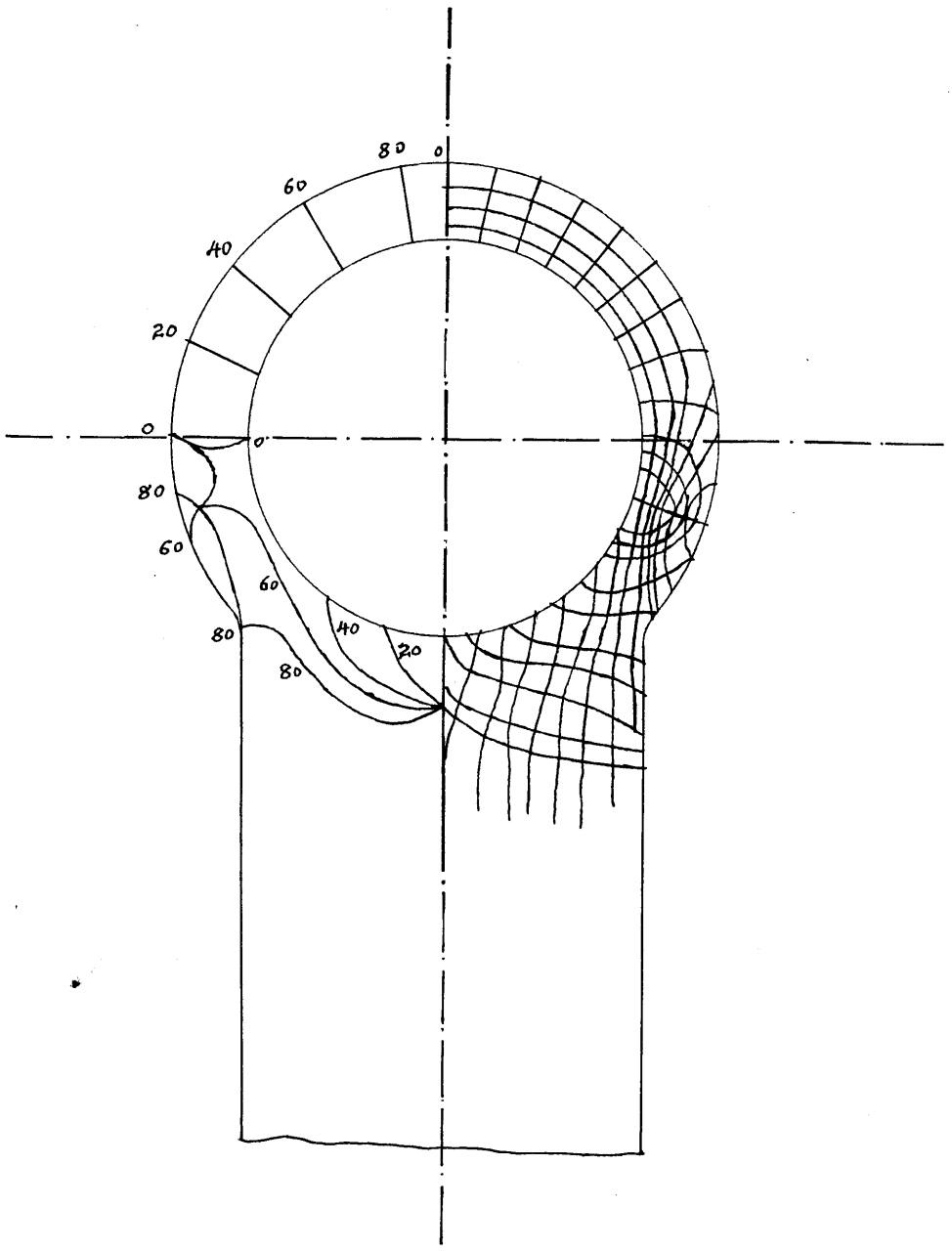

FIG. 7

MIDDLE STRIP

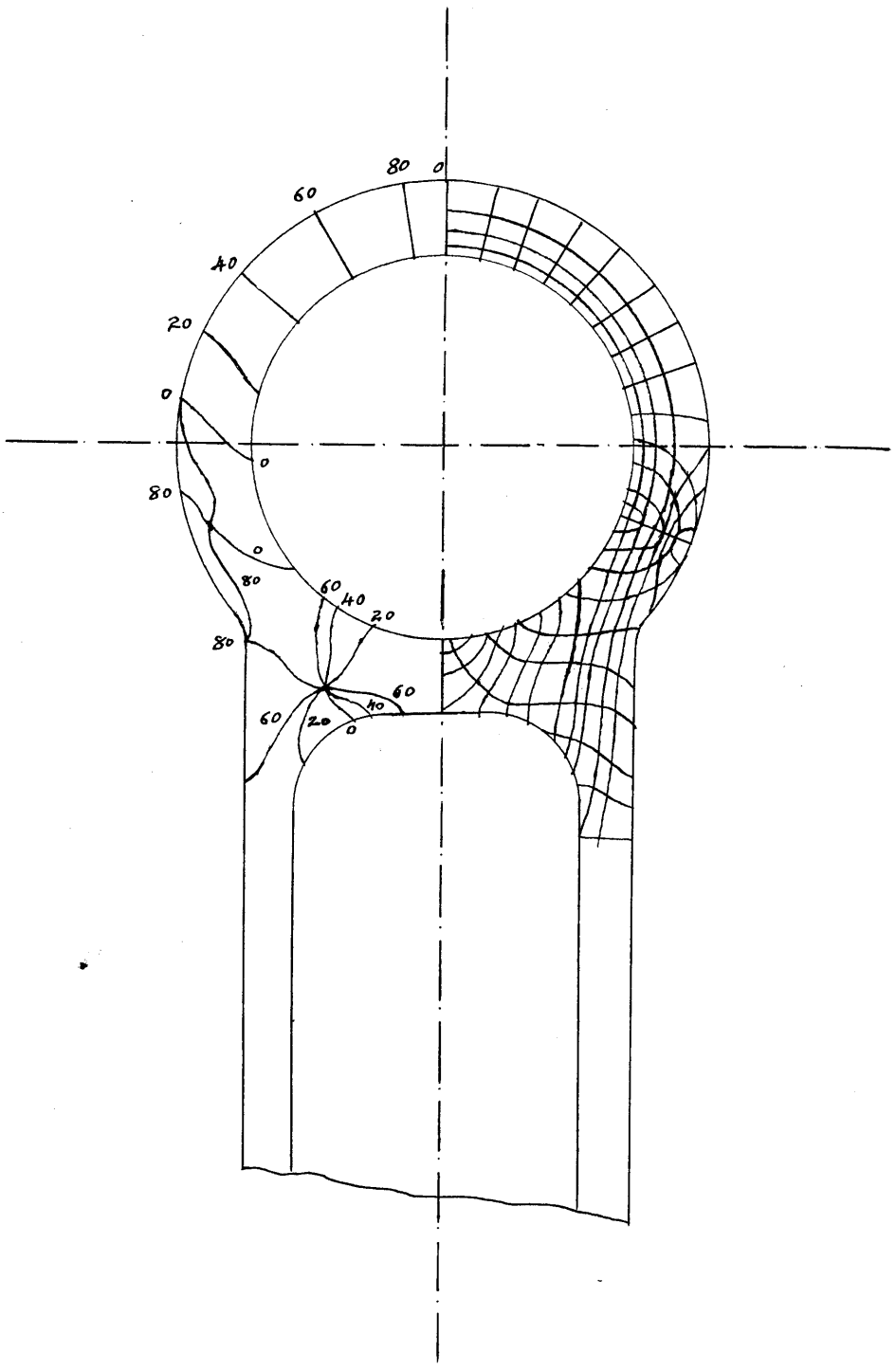

FIG. 8

SIDE STRIP

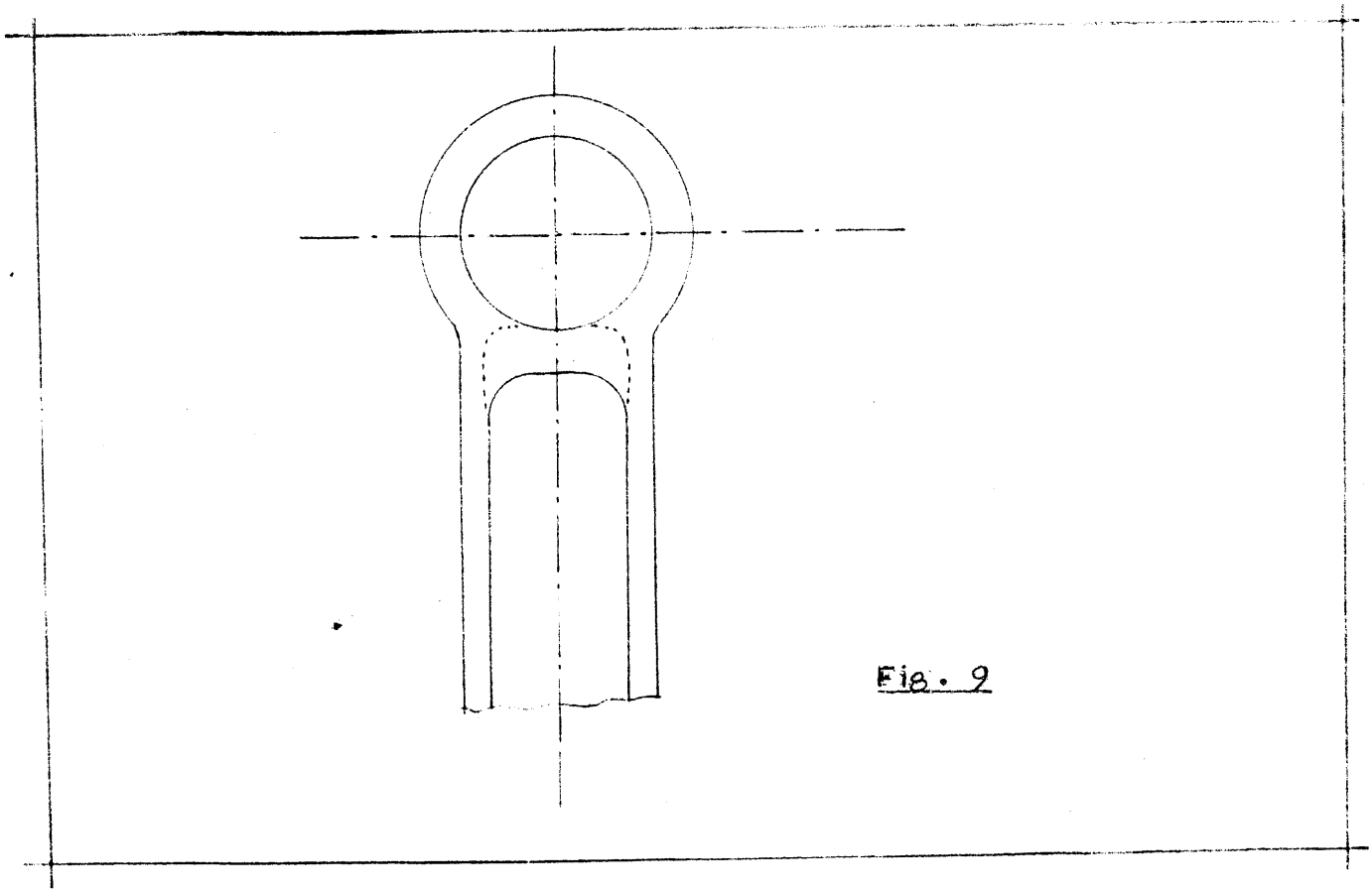

Fig. 9

From these results we see that the stress variation in the middle strip will not be very different from that in the side strip.

If we study the stress trajectories for these sections (Fig. 7 and 8), we see that the direction of the principal stresses in the eye-ring section of the connecting rod are the same in both the strips, Fig. 7 and 8. The only change that takes place is in the region just below the lower part of the inside edge. Fig. 7 and 8.

After the study of the p-q curves and the stress trajectories and the isoclinics for these two strips, the author has come to the conclusion that the only variation that must be taking place must be somewhere in the region shown by the dotted line in figure 9. Now from the lacquer experiment and also from the two dimensional results, it was found that this region is subjected to a very low stress. In his experiment in lacquer, the author painted the model with a lacquer layer and allowed it to dry. After the lacquer was completely dry, the author loaded the model with a load of 390 lbs. It was observed that no cracks appeared in the region shown by the dotted lines in Fig. 9. The author wanted to confirm whether the absence of cracks was due to a compressive stress or was due to the fact that the region was not subjected to an appreciable stress at all, so he kept the model loaded for 6 hours and then unloaded the model. It was observed that not a single crack appeared even after

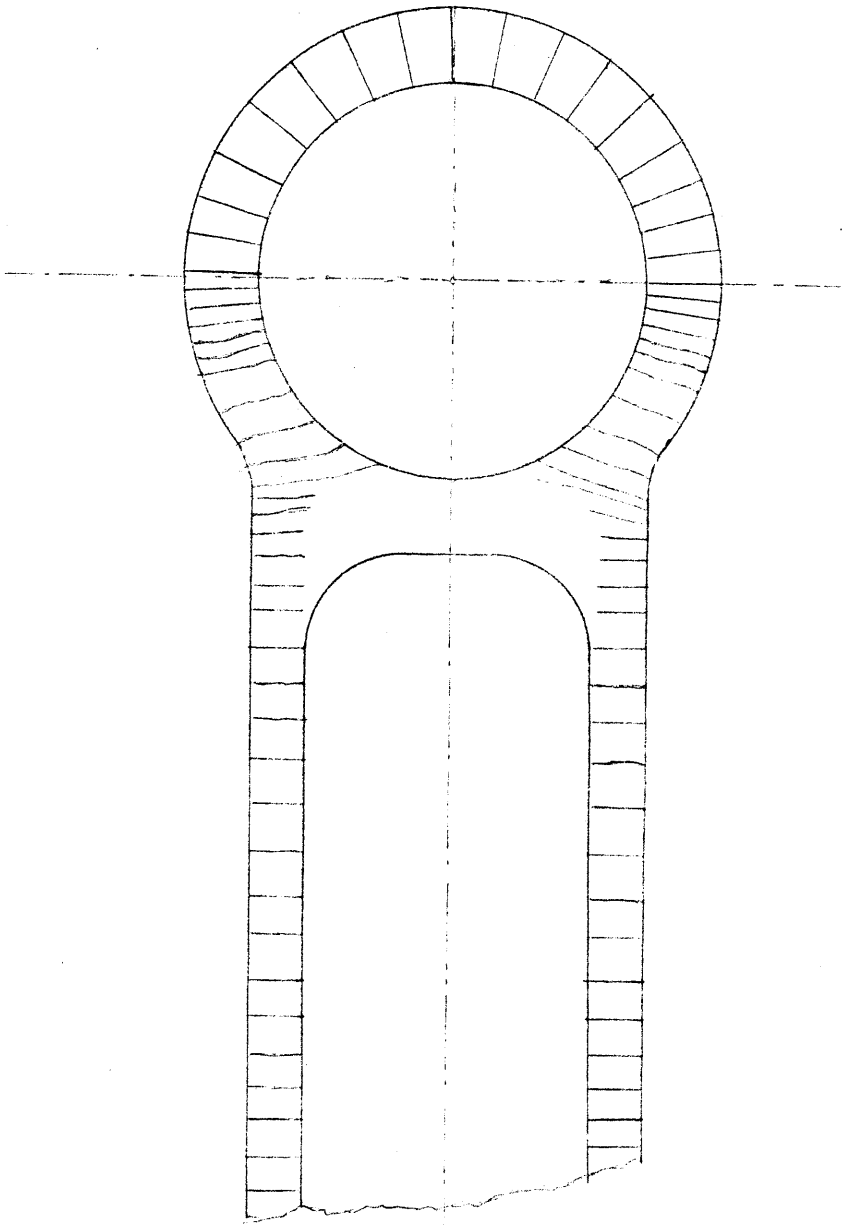

The cracks obtained during the Lacouer Experiment.

Fig. 10

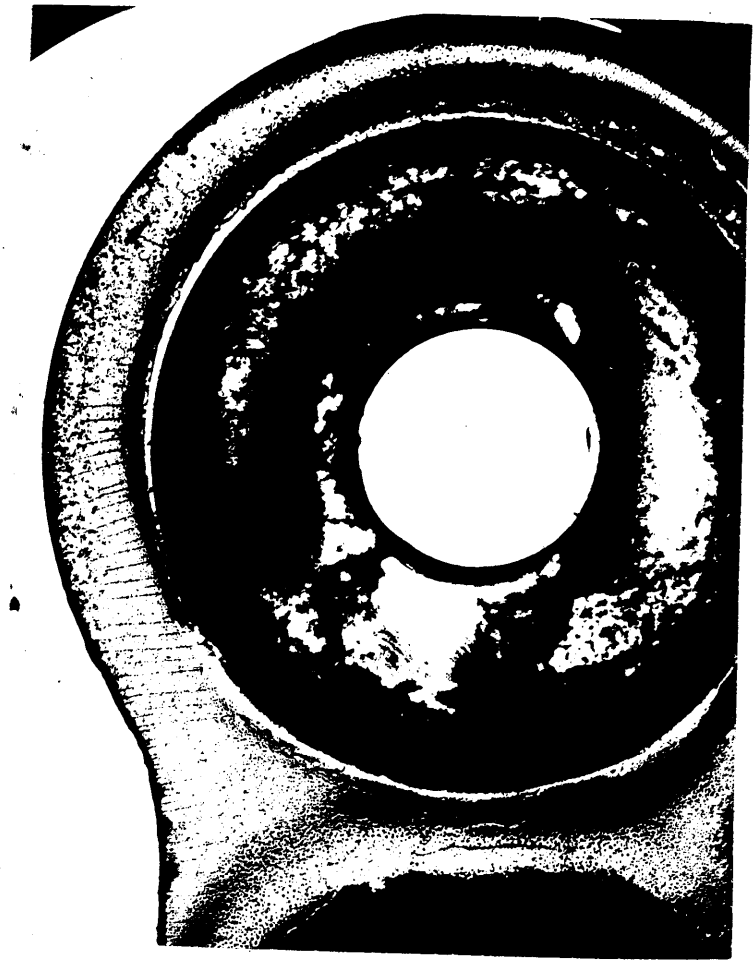

FIG. 11

FIG. 12

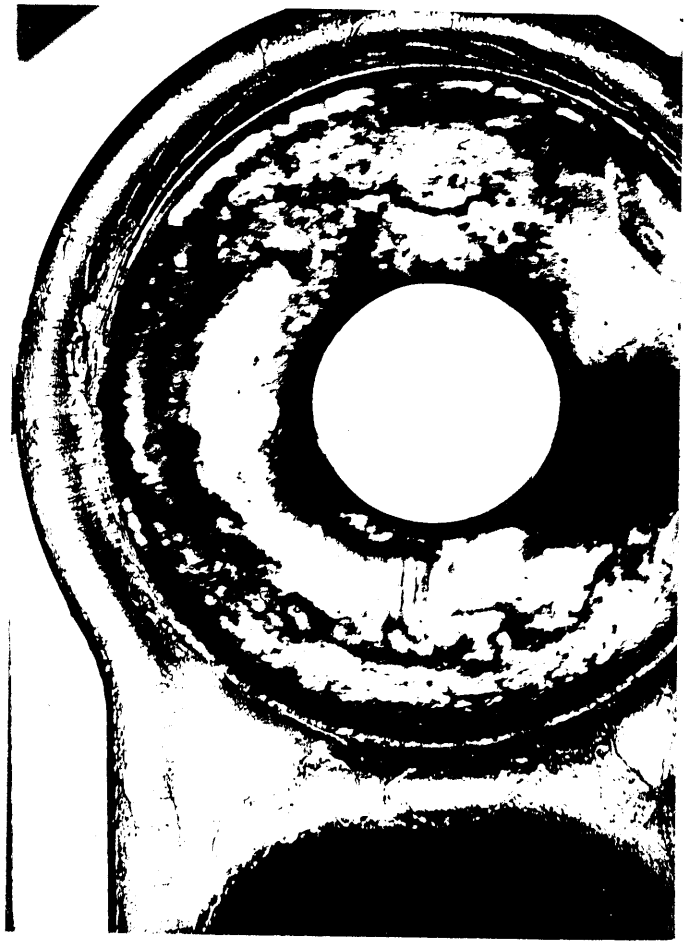

FIG. 13

FIG. 14

FIG. 15

that treatment and so the author concluded that the absence of the cracks was due to the fact that the region concerned was subjected to a stress which was very low in value.

The photographs obtained in the lacquer experiment are given on Figs. 11 to 15 and Fig. 10 gives a general view of the cracks that appeared on the lacquer due to loading.

The model of the connecting rod was very small and it was very difficult to get a better picture of the cracks. The author hopes that Fig. 10 will give a clear idea about the cracks which were quite visible on the model.

From the above discussion the reader will understand how in the three dimensional treatment the stress concentration in the eye ring portion will remain the same for both the strips. The author came to the conclusion that, for the three dimensional treatment was not necessary in the case of a connecting rod.

Two-Dimensional Method

In his experiments, in two dimensions, the author studied the sections AA and BB (Fig. 1) and found out the actual values of the principal stresses p and q for these two sections, thinking that the maximum stress concentration would occur somewhere on these two cross-sections. The complete stress analysis of these two sections was obtained from the p-q and p+q curves for these two sections. The detail analysis and the results will be given on the next pages.

After the mathematical study of the subject, the author has realized that his assumption that the maximum stress would occur on the section AA was not correct. The position of the e section on which the maximum stress would occur depends on many variables, which will be discussed in detail at the end of this paper. So it will be seen that, though the author has studied the stresses in two of the principals sections, the work is still incomplete even from the point of view of maximum stress concentration, and there is a vast field for the other investigators.

Before giving the results of the experiments and tables, the author would like to describe in short, the method of his experiments and the precautions that he had to take during the experiment. Of course, the reader is here supposed to have a general knowledge of the apparatus of the photoelasticity and the strain gages.

The author fitted a pin inside the eye, the former being made of the same material as that used in the construction of the connecting rod. (Bakelite BT 61-893). A steel rod was inserted through the middle of this pin to help hold the whole structure in the loading machine.

This precaution of keeping the pin of the same material as that used in the connecting rod body is very essential, because as the reader would see, from the photographs taken during the three dimensional treatment, (Fig.5,6) the eye-hole of the connecting rod becomes elliptical when

the rod is loaded. Though the deformation obtained in this way, in the three dimensional treatment, is much more exaggerated of form, it gives a very good idea of the way in which the eye of an actual connecting rod would deform. Now in the case of a Bakelite model of the connecting rod, if we use a steel pin while loading, the manner in which the eye section deforms would be completely changed, and consequently, the stress distribution also will be changed, therefore, the author is of the opinion that the pin used must be made of the same material.

(b) The loading arrangement must be such that the connecting rod is loaded exactly vertically and has no bending moment whatsoever. This was obtained in the present case by using two universal joints, one at each end.

(c) The amount of load that one should put depends on the material used, and also on the size of the enlargement of the fringe photograph. In the present case, the author obtained a fairly good pattern with a load of 152.5 lbs.

(d) The pin was introduced inside the eye, with a slight force. This question of "fit" is a debatable one, and as will be seen later, from the discussion of the results, the manner of "fit" plays a very important part in the position of the stress concentration.

In case of an actual connecting rod, one knows, that the pin is a "slide fit"and not the"force fit." So, one may argue, that during the experiments, one must not use a "force fit". The author thinks that, as the eye-holes are fitted generally with a bushing made of some kind of bearing material, the manner of "fit" depends on the manner of fit

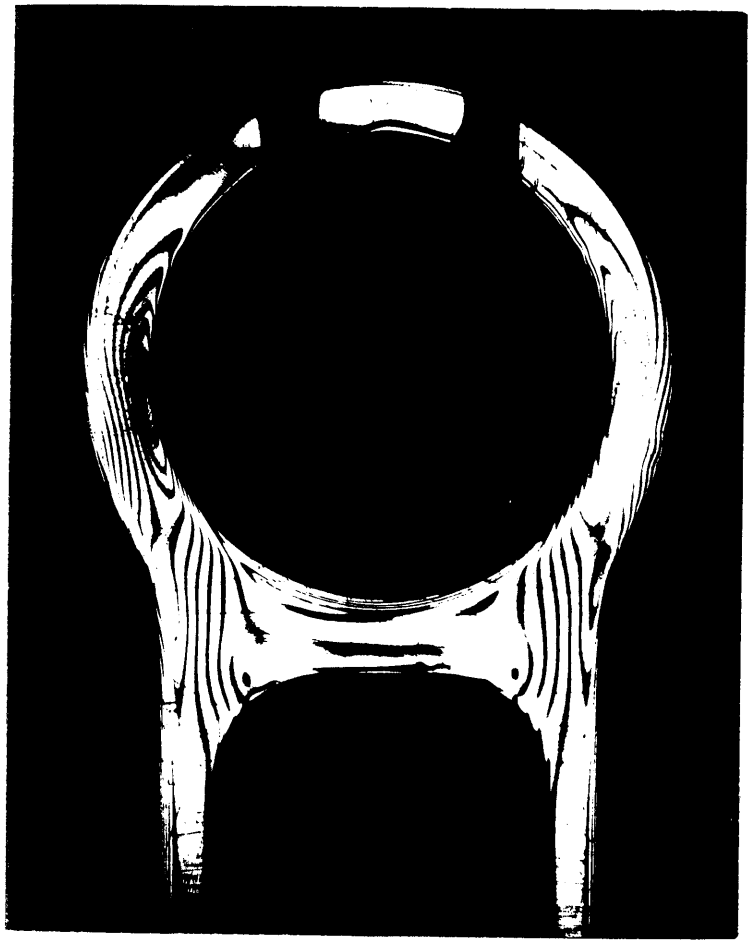

FIG. 15 A

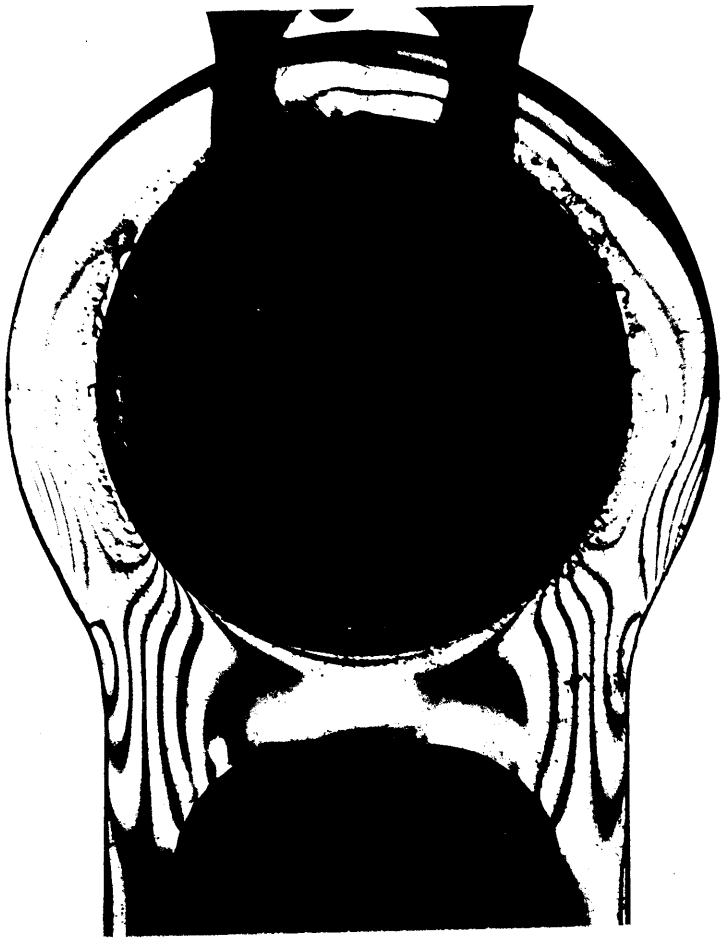

FIG. 15 B.

TABLE 1

Distance from the outside edge	Fringe order	(p-q) Lbs/a "
0	11	1290
.0145	10	1170
.029	9	1050
.051	8	935
.062	7	820
.076	6	700
.094	5	534
.113	4	467
.130	3	350
.145	2	234
.159	1	117
.174	0	0
.188	1	117

Table 2

THE VALUES OF p AND q OBTAINED
FROM
THE(p-q) and (p+q) CURVES :

Stations	(p-q) Lbs/□"	(p+q) Lbs/□"	p Lbs/□"	-q Lbs/□"
0	1350	235	792.5	557.5
.5	1140	290	715	425
1.0	1005	340	672.5	332.5
1.5	880	385	632.5	247.5
2.0	760	430	595	165
2.5	635	470	552.5	82.5
3.0	510	498	504	6
3.5	380	480	430	- 50
4.0	260	430	345	-85
4.5	130	355	242.5	-112.5
5.0	0	250	125	-125
Edge	117	117	117	0

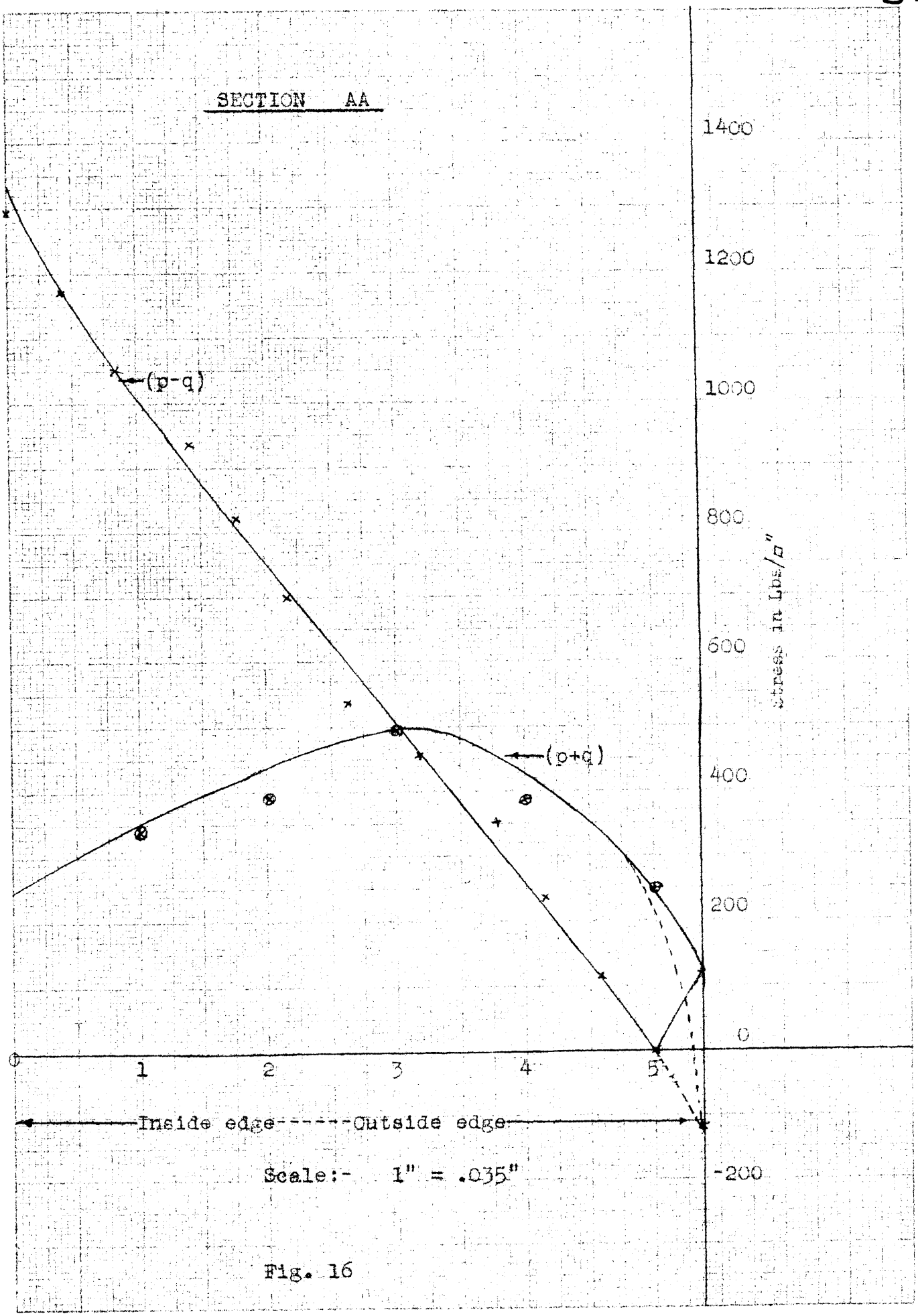
SECTION AA
1400
1200
1000
800
600
400
200
0
-200
(p-q)
(p+q)
Stress in Lbs/□"
0
1
2
3
4
5
Inside edge------Outside edge
Scale:- 1" = .035"

Fig. 16

of this bushing, and not on that of the pin itself. Because of this reason, the author has used a "force fit" and not a "slide fit" in this experiment.

(e) It was observed by the experiments that a slight oil film on the pin gives a much better uniform loading and consequently a better fringe picture.

Results:- (Experimental)

The Figs. 15A and 15B shows the fringe photographs obtained during the experiment, the latter being taken on the light field. The Tables 1 and 2 gives the p-q and $(\phi+\psi)$ values for the section AA (Fig. 1) obtained from the fringe photographs. The graph in Fig. 16 shows this curve.

Note: Here the reader is asked to note the two different ways of plotting the (p-q) curves. (one shown by the dotted curve). The question in this case is about the existence of a singular point on the section AA.

From the lacquer pattern that the author obtained, it was quite obvious that the section was not subjected to a compressive stress and consequently, there could not be a singular point on the section. The mathematical treatment showed that the section concerned is subjected to a compressive force and so the author has drawn two alternative curves. The curves in Figs. 18 and 19 for p and q are also shown in the two different ways, each representing the corresponding p-q curve.

TABLE 3

READINGS OF THE INTERFEROMETER FOR THE SECTION AA:

STATION 1		STATION 2		STATION 3	
Load in Lbs	Lines	Load in Lbs	Lines	Load in Lbs	Lines
116	0	67	1	55	0
128	1	75	2	62	1
140	2	85	3	69	2
150	3	94	4	77	3
157.5	4	104	5	84	4
169	5				

STATION 4		STATION 5	
Load in Lbs	Lines	Load in Lbs	Lines
65	0	74	0
72.5	1	88	1
83.5	2	1o2.5	2
92.5	3	117	3
102.5	4	128	4

TABLE 3a

(p+q) values for the section AA

Station	Δ bands	(p+q) lbs/□''
1	14.3	336
2	16.5	388
3	20.9	491
4	16.5	388
5	10.5	246

where $(p+q) = \frac{\Delta h \times E}{h \int N}$

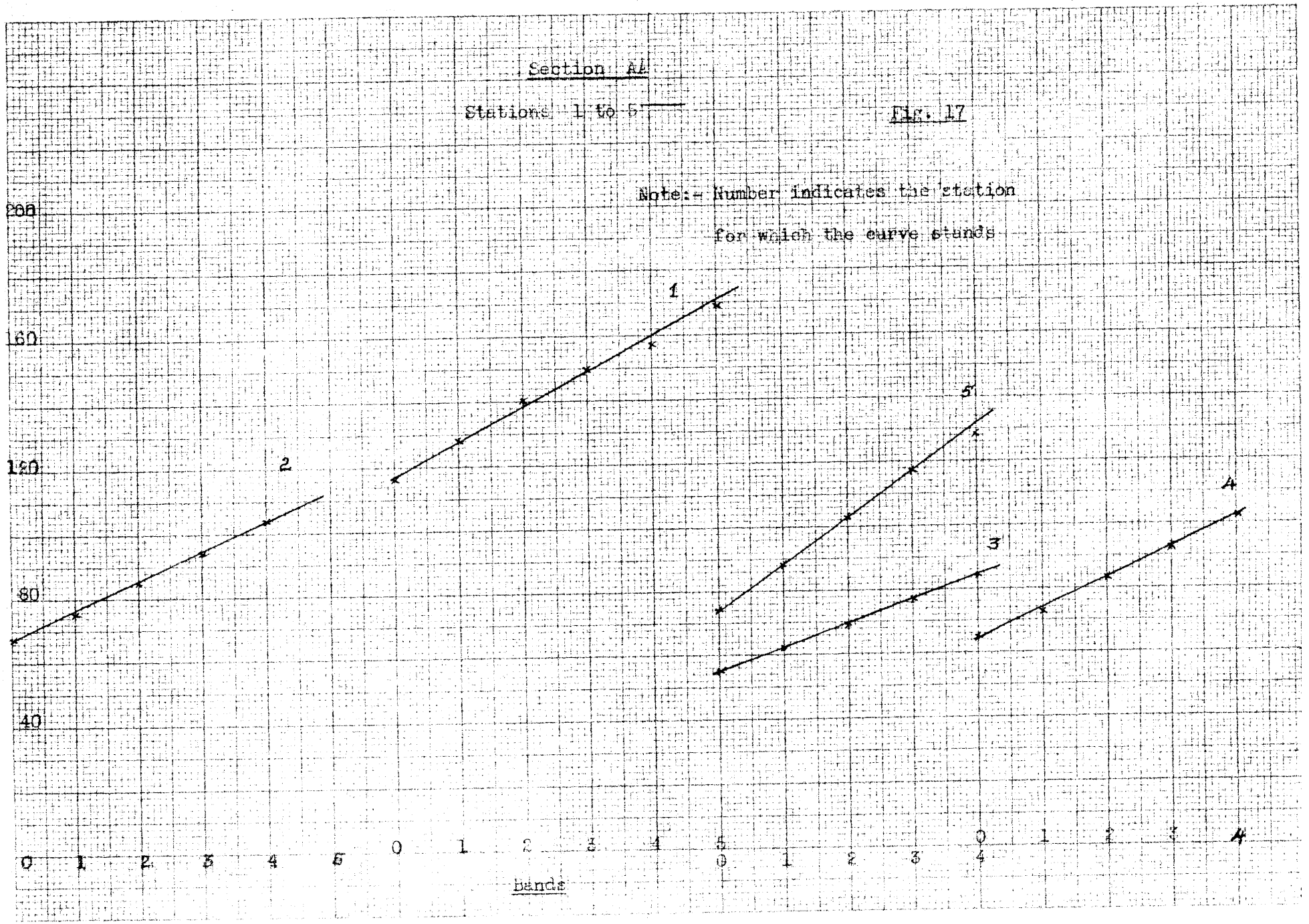
Section AA
Stations 1 to 5
Fig. 17
Note:- Number indicates the station for which the curve stands
200
160
120
80
40
Load in Lbs.
1
2
3
4
5
0 1 2 3 4 5
0 1 2 3 4
0 1 2 3 4
Bands

For finding the (p + q) value for this section, five stations were located on this section and the interferometer strain gage was used to determine the change in the strain for each point. The change in load required for the change in every interference line was noted. (the Table 3 and 3a gives these values). These values give an almost straight line curve for each point. A separate graph was plotted for each point and the bands for a load of 152.5 lbs. was calculated from the slope of this graph. The graphs in Fig. 17 show the curves for this station.

From these values of bands for each point, the p+q value for that point was calculated by the use of Lateral Constant (Note: the Lateral Constant for the material was found by the usual experiments, but for the sake of brevity the author does not propose to give in detail the experimental results and graphs obtained in this experiment. The Lateral Constant was found to be 17.3)

The curve of p+q for this section AA is drawn in Fig. 16. From these two curves of p-q and p+q, the separate curves of p and q were plotted as shown in Figs. 18 and 19.

Now the lacquer pattern obtained to get the stress trajectories show that the direction of the principal stresses (p and q) at the section AA are exactly tangential and radial (Fig. 10), so in this case, the load obtained by integrating the p curve must give the value = $\frac{P}{2}$, where P is the total load applied on the model. This was checked and found that the

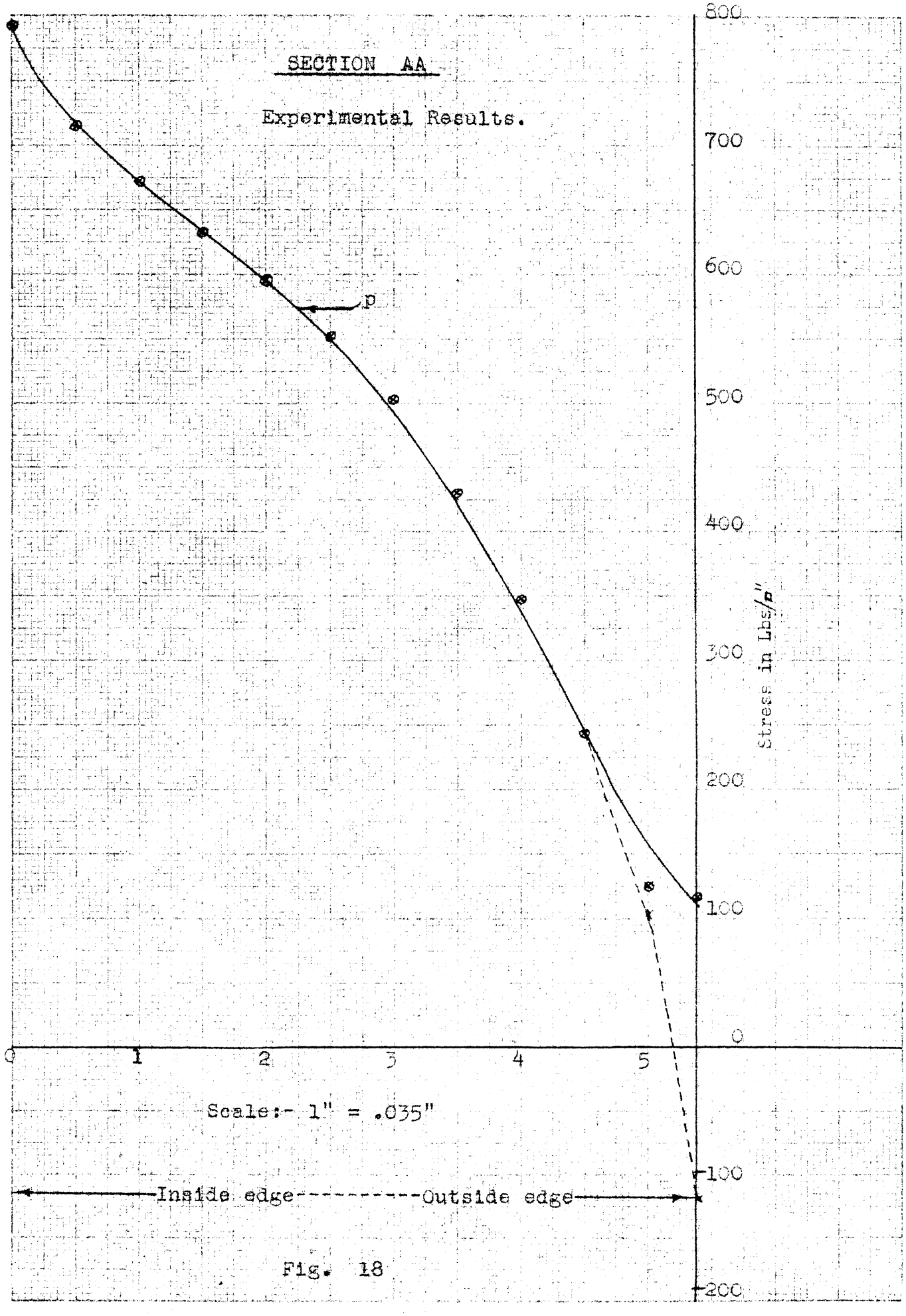
SECTION AA
Experimental Results.
800
700
600
500
400
300
200
100
0
-100
-200
p
Stress in Lbs/"
0
1
2
3
4
5
Scale:- 1" = .035"
Inside edge----------Outside edge

Fig. 18

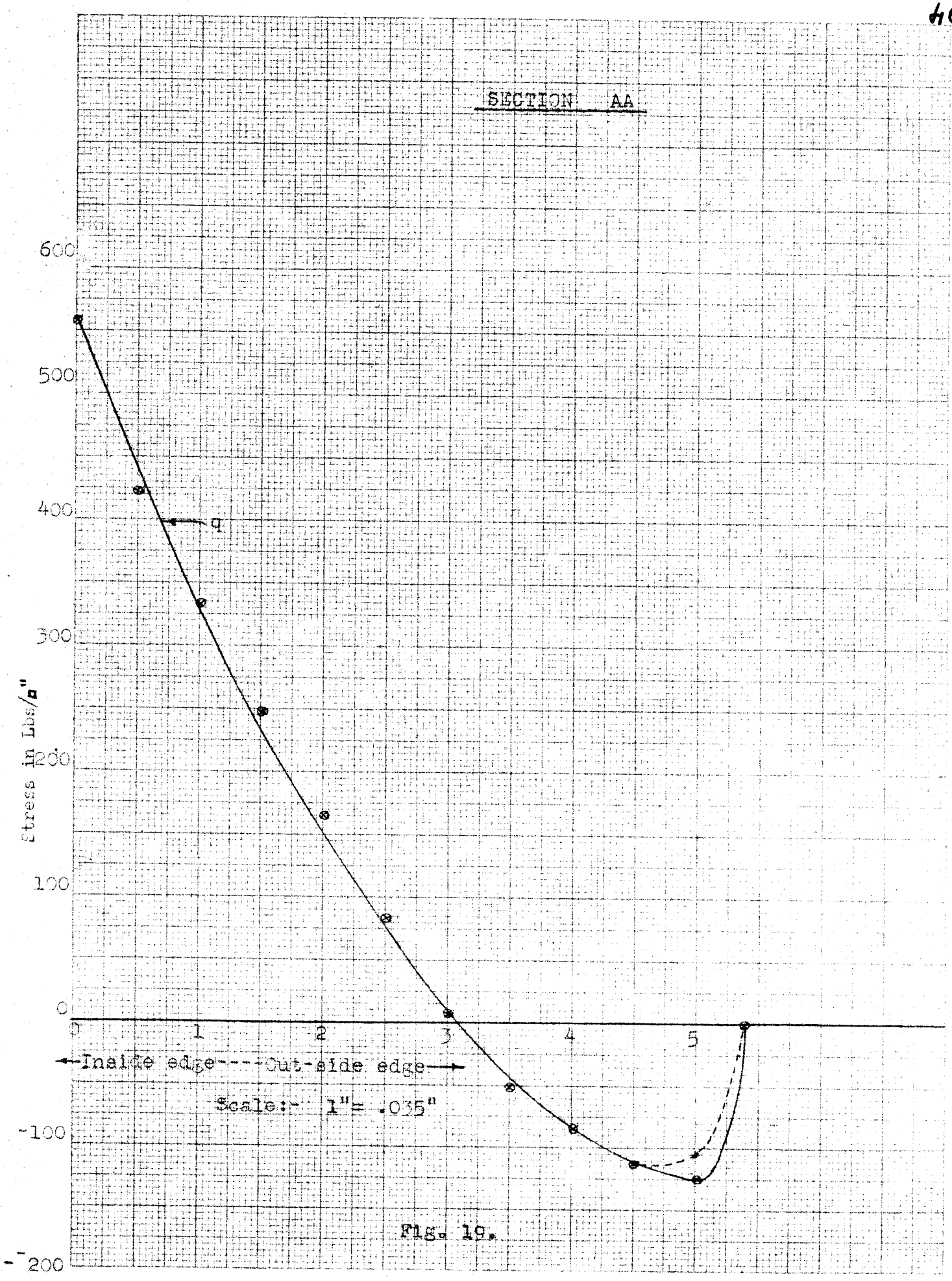
SECTION AA
600
500
400
300
200
100
0
-100
-200
Stress in Lbs/□"
q
0
1
2
3
4
5
←Inside edge---Out-side edge→
Scale:- 1" = .035"

Fig. 19.

Table ---4

The values of (p+q) for the

Section BB

Stations	Distance from the outside-edge.	Bands for a load= 152.5Lbs.	(p+q) Lbs/a"
1	.03	17.95	421
2	.0925	15.25	358
3	.155	7.75	182
4	.2175	3.72	87.5
5	.28	3.6	84.6
6	.3425	5.25	123.5
7	.405	4.36	102.5
8	.4675	3.99	93.8
9	.53	4.8	113

The values of (p-q) for the

Section BB

Points	Distance from the outside-edge	Number of order	(p-q) lbs/a"
1	.00444	5	585
2	.0178	6	700
3	.0488	6	700
4	.0666	5	585
5	.089	4	467
6	.115	3	350
7	.151	2	234
8	.195	1	117
9	.32	1	117

Table---5

p and q values for the Section BB--

Distance from the outside edge.	(p+q) Lbs/in	(p-q) Lbs/in	p Lbs/in	-q Lbs/in
0.000	520	520	520	0
.025	465	715	590	125
.050	410	700	555	145
.100	305	410	357.5	52.5
.150	200	230	215	15
.200	100	115	107.5	7.5
.250	85	100	92.5	7.5
.300	87	115	101	14
.350	90	125	107.5	17.5
.400	95	130	112.5	17.5
.450	97	132	114.5	17.5
.500	102	135	118.5	16.5

error was only 10.8% of the correct load, which is a quite satisfactory result for the photoelastic work.

Calculations:-

Area under the p curve = 26.125 sq. in.(Not the dotted curve)

The scale for the abscissa ----1" = .035"

The scale for the ordinate --- 1" = 100 lbs.

So 1 square inch = 3.5 lbs/inch thickness of the model.

Total load = 2x(26.125 x 3.5x .744)

= 136 lbs.

$$\% \text{ error} = \frac{152.5 - 136}{152.5} = .108 \text{ i.e. } \underline{10.8\%}$$

The stress concentration for this section, compared with the mean stress across this section will be as follows:

Actual maximum stress obtained by experiments = $p_{max.}$ = 792.5 lbs. per sq. in.

$$p_{mean} = \frac{152.5}{2 \times .188 \times .744} = 546 \text{ lbs/per sq. in.}$$

So the stress concentration $= \frac{792.5}{546} = \underline{1.45}$

Section BB (Fig. 1)

The Table 4 gives the p-q values and the distances of those points for the section BB. Here the curve is drawn only for half the section, the remaining half being the duplicate of this curve.

Section BB

Stations 1 to 9

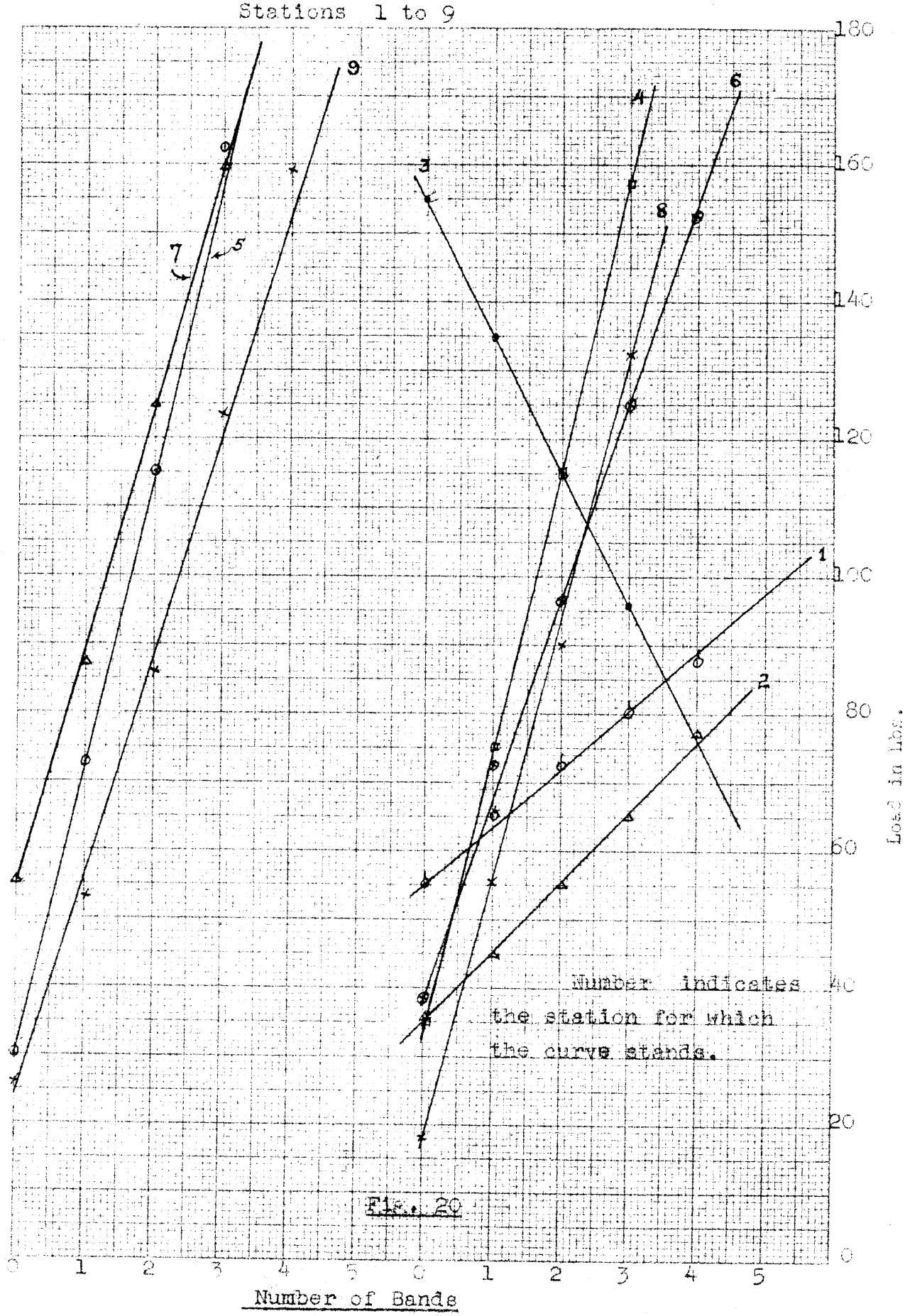

Fig. 20

TABLE 6

STRESS- VARIATION ALONG THE EDGE OF THE CONNECTING ROD.

Distance from the head of the eye-section in inches	Order of Number	Stress p Lbs/$\square$"
.0889	4	468
.311	3	350
.506	2	234
.58	1	117
.666	2	234
.835	3	350
.940	2	234
.995	1	117
1.040	2	234
1.065	3	350
1.091	4	468
1.155	5	585
1.215	4	468
1.28	3	350
1.350	2	234
1.44	1	117

TABLE 7

READINGS OF THE INTERFEROMETER FOR THE SECTION BB

STATION 1		STATION 2		STATION 3	
Load in Lbs	Lines	Load in Lbs	Lines	Load in Lbs	Lines
55	0	36	0	155	0
65	1	45	1	135	1
72.5	2	55	2	115	2
80	3	65	3	96	3
87.5	4	77.5	4		

STATION 4		STATION 5		STATION 6	
Load in Lbs	Lines	Load in Lbs	Lines	Load in Lbs	Lines
35	0	30	0	38.5	0
75	1	72.5	1	72.5	1
115	2	115	2	96.5	2
157.5	3	162.5	3	125	3
				152.5	4

STATION 7		STATION 8		STATION 9	
Load in Lbs	Lines	Load in Lbs	Lines	Load in Lbs	Lines
160	3	18	0	26	0
125	2	55.25	1	53	1
87.5	1	90	2	86	2
55	0	132.5	3	123.5	3
				159	4

(p-q) and (p+q) curves for the section BB

Fig. 21

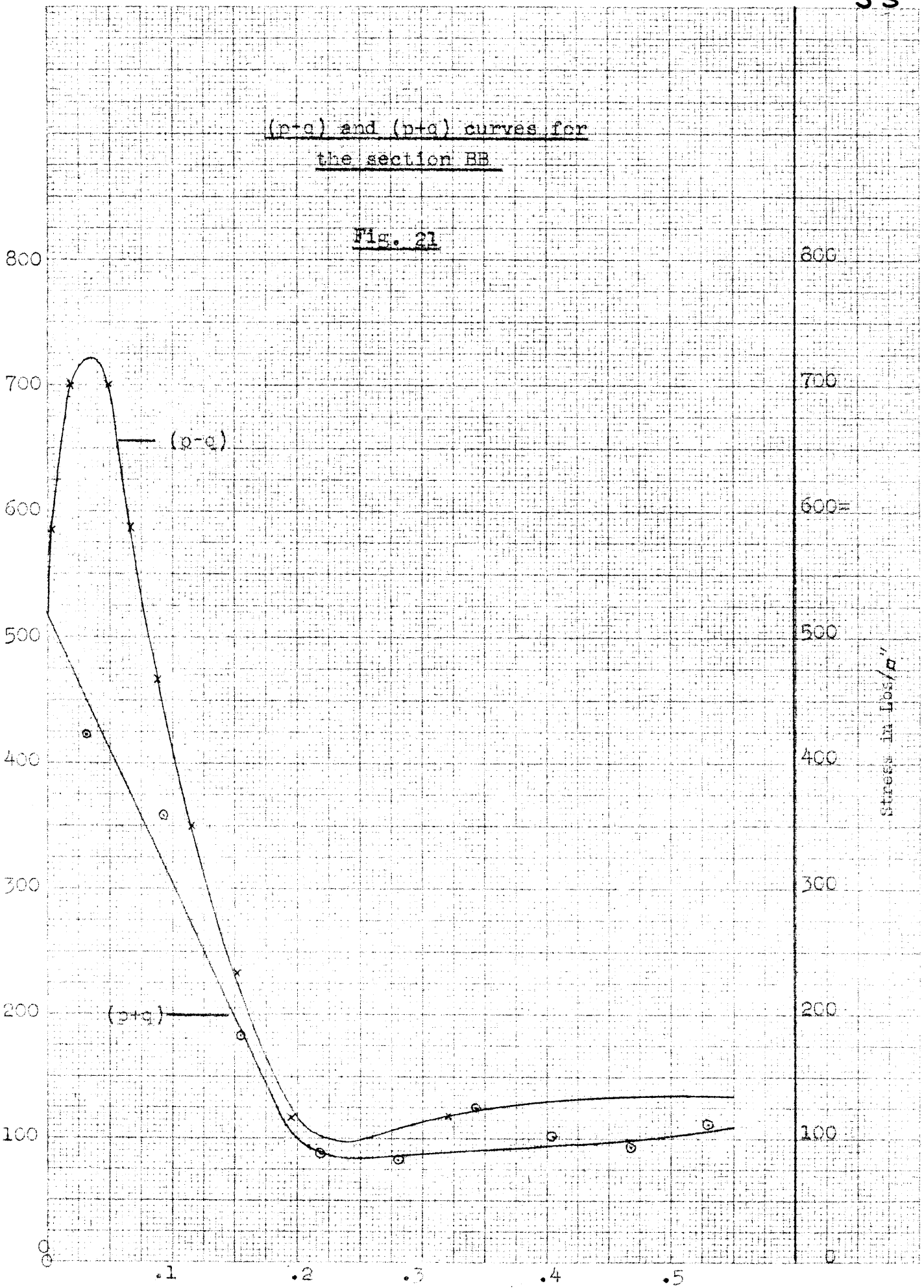

Distance from the outside edge in inches.

p and q curves for

Section BB

Fig. 22

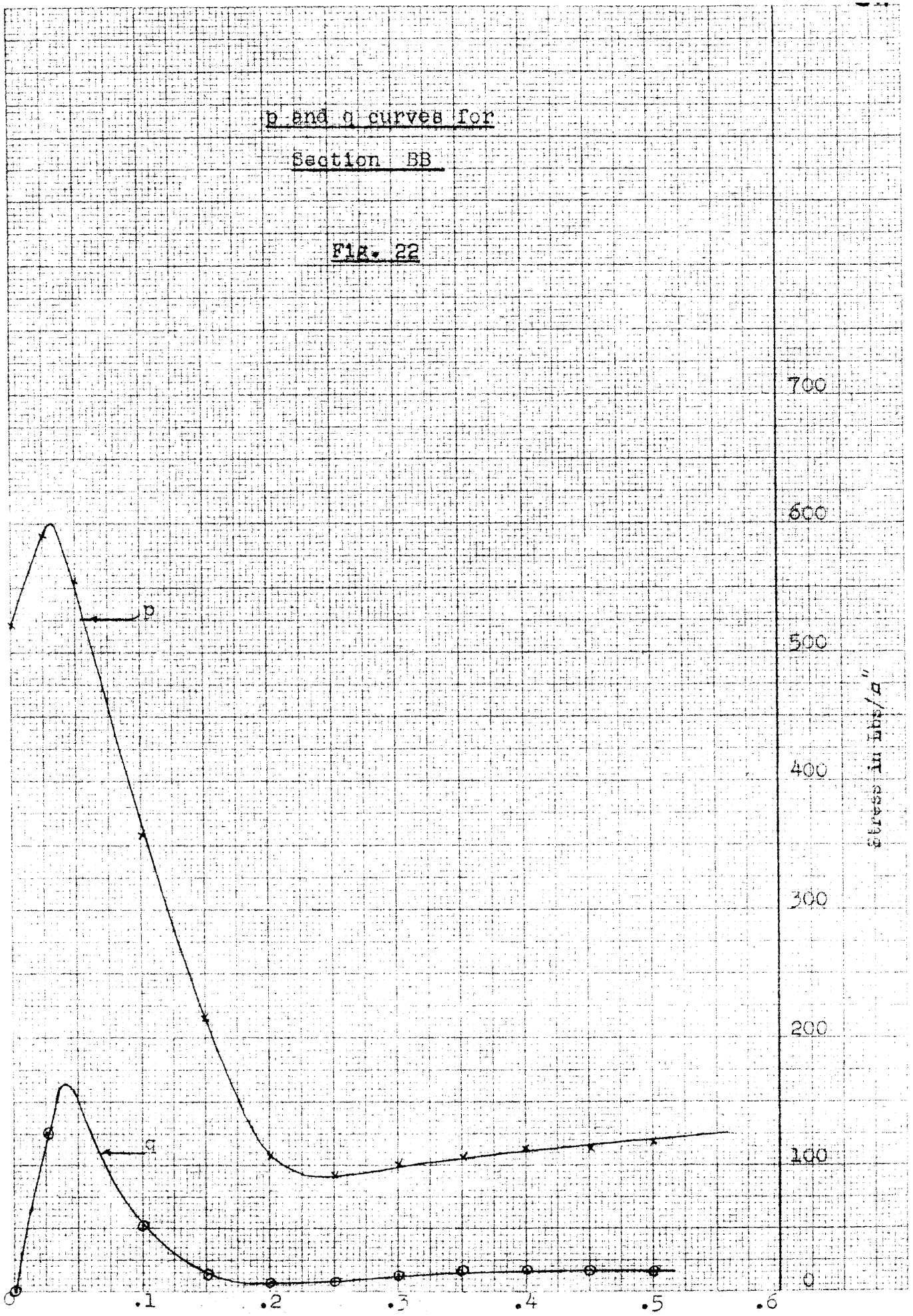

Distance from the outside edge in inches.

The Tables 4 and 5 give similarly the values of p+q obtained exactly in the same manner as described above. 8 sections were located on this section. The curves in Fig. 20 show the Δ bands against the load for each station. And Table 7 gives these values.

The values of p-q and p+q were plotted as usual in Fig. 21 and from that the p and q stresses were evaluated and plotted on a separate graph, Fig. 22.

For this section too, one sees from the lacquer pattern that the direction of the principal stresses is almost horizontal and vertical (considering the main axis of the connecting rod as vertical). So in this case too, the load obtained from the area of the p curve must be $= \frac{P}{2}$ (because our curve is only for half the section across BB).

Calculations:-

Scale for abscissa = 1" = .1"

" " ordinate = 1" = 100 lbs/ sq. in.

Area under the curve = 10.625 sq. in.

One square inch = .1 x 100 = 10 lbs/inch width of the model.

Thickness of the model = .744

$\therefore$ Load = 10.625 x .744 x 10 x 2 = 158 lbs.

$\therefore$ Error = $\frac{158 - 152.5}{152.5}$ x 100 = 3.4%

Here, the error is very small and the results are

Stress Variation at the outside edge of the connecting rod

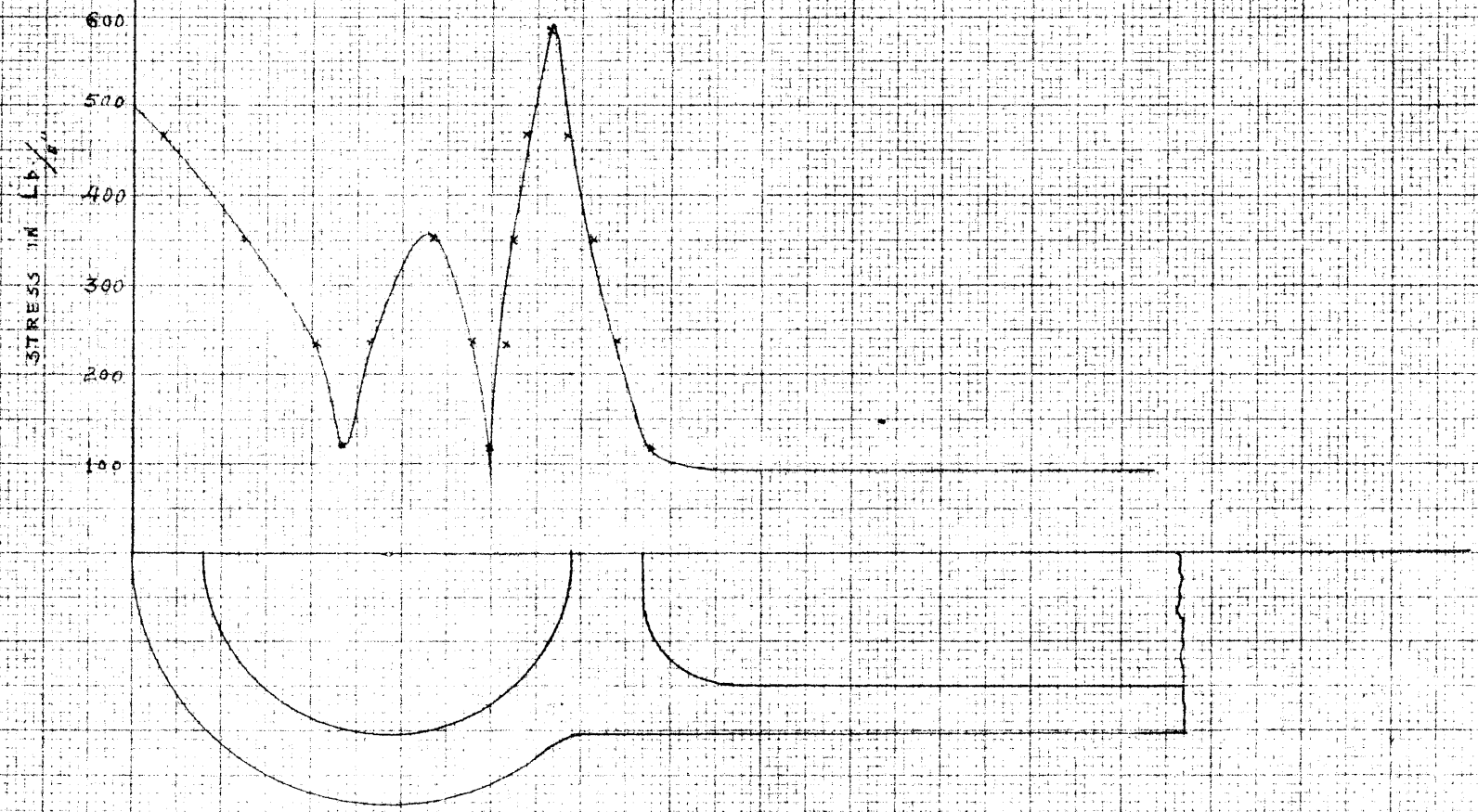

Scale double size

Fig 23

amazingly accurate.

Coming to the third curve in our experiment, the author calculated the stress variation across the outside boundary of the connecting rod from the fringe photographs of the model. (Fig. 15A and 15B). As is well known - one of the principal stresses at the boundary is zero and the fringe pattern gives directly the stresses at those points. The value of these stresses and the distance of the points were tabulated (Table 6) and plotted as shown in Fig. 23. This curve gives a very good idea about the stress variation along the outside boundary of the connecting rod.

Coming to the last experimental curve in this paper, Fig. 24 shows a curve across the section CC (1). Here too, the load being vertical and one of the principal stresses being vertical too, the stress q will be 0, and so the fringe photographs will give directly, the value of the other principal stress, i.e., p. This curve is drawn in Fig. 24.

Mathematical Calculations:-

For his problem, the author of this paper studied the mathematical treatment discussed by Mr. H.Reissner of Berlin, in "Jahrbuch, der Wissenschaftlichen, Gesellschaft fur Luftfahrt e.V.(WGL) 1928, and has used the same method to calculate the stresses for his connecting rod. So the reader would see that the method given below is just copied

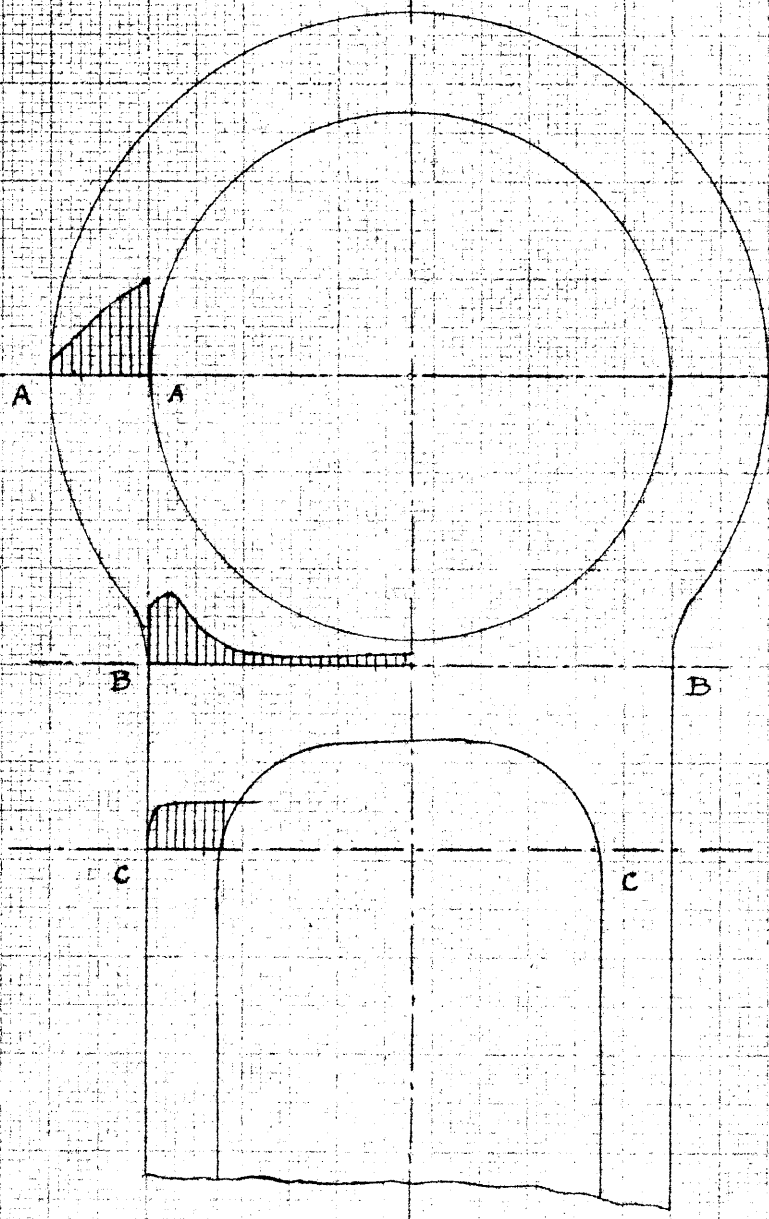

Scale:- 1"= .375"

Scale for the stress curve:-

1"= 1600 Lbs/$_{\square}$"

Fig. 24

from the above paper. The author of the present paper has given the theory in detail on the fond hope that some other investigator would take up the problem in future and would be benefited by it.

Fig. 25 gives the curve obtained from the mathematical calculations:

In this case the integration of the p curve must give a total load which will be equal to $\frac{p}{2}$. The calculations are as follow:

Data:-

The area of the curve (mathematical curve) in Fig. 25 = 7 - 2.25 = 4.75 sq.in.

Scale of the abscissa = 1" = .0376"

" " " ordinate = 1" = 600 lbs/sq.in.

$\therefore$ 1 square inch = .0376 x 600 = 22.56 lbs/inch width

$\therefore$ Total load = 2 x 22.56 x 4.75 x .744 = 159 lbs.

$\therefore$ % Error = $\frac{159 - 152.5}{152.5}$ x 100 = 4.27%

The Fig. 25 gives the curve obtained from the mathematical calculations.

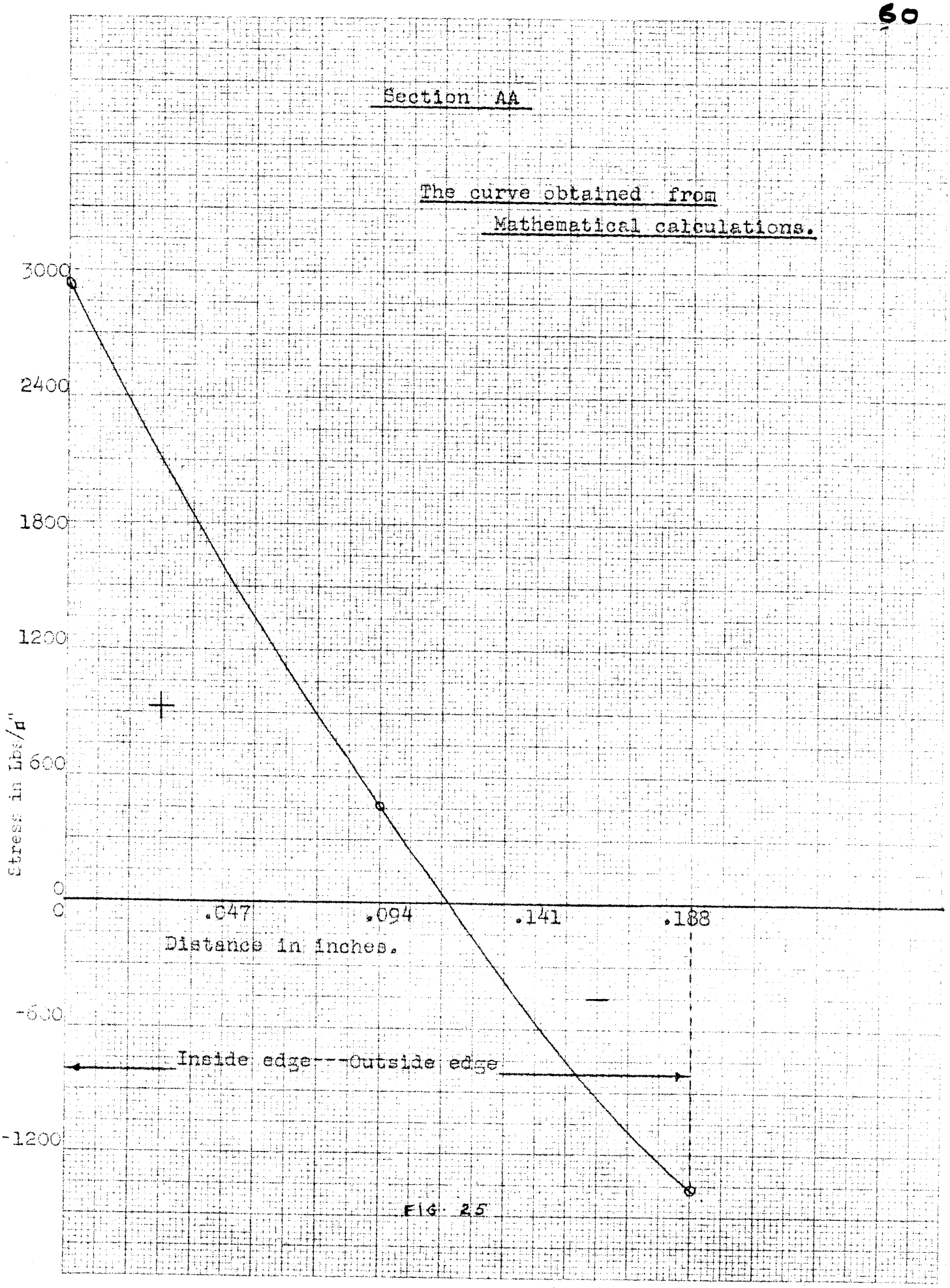
Section AA
The curve obtained from
Mathematical calculations.
3000
2400
1800
1200
600
0
-600
-1200
Stress in Lbs/sq"
0
.047
.094
.141
.188
Distance in inches.
+
−
Inside edge---Outside edge

FIG 25

MATHEMATICAL SYMBOLS

u or v = Radial or Tangential Displacement

ν = Normal Stress (Positive when in Tension)

ν_r = Radial Stress (Ring Stress)

ν_θ = Tangential Stress

τ = Shear Stress

ε = Unit Elongation

ε_r = Radial Elongation

ε_θ = Tangential Elongation

γ = Change in Angle

E = Modulus of Elasticity

μ = Poisson's Ratio

δ = Thickness ofthe plate of the Ring

r_a and r_i = Outside and Inside Radii of the Ring

α and β = Coefficient of the development of the series for obtaining u and v shown by the constants $a_1^{(n)}\ a_2^{(n)}\ a_3^{(n)}\ a_4^{(n)}$ and similarly for β

$\delta_1^{(n)}\ \delta_2^{(n)} \ldots$ = Coefficients for the development of a series for the stresses ν and τ shown by $\delta_1\ \delta_2\ \delta_3 \cdots$ etc.

P = Total resultant force

ν_m = Mean Stress = $\frac{P}{2(r_a - r_i)\delta}$

ν_l = Average Ring Stress = $\frac{P}{2 r_i \delta}$

$$\eta = \frac{r_i}{r_a} \; ; \quad \lambda = \frac{1}{\eta} = \frac{r_a}{r_i}$$

$$\gamma_i = \frac{r_i}{r} \; ; \quad \gamma_a = \frac{r}{r_a}$$

$$\nu_\theta' = \nu_\theta \frac{\pi^2}{8} \frac{r_a \delta}{P} = \frac{\nu_\theta}{\nu_l} \cdot \frac{\pi^2}{16\eta} = \frac{\nu_\theta}{\nu_m} \frac{\pi^2}{16} \frac{1}{1-\eta}$$

The ~~Method~~ Mathematical Theory

The well-known fundamental equations for the plane problem of a ring-shaped plate are given below in the cylindrical polar coordinate form. The equations are obtained from the equilibrium condition for the normal stresses σ_r and σ_θ and shear stress τ. (Fig. Ma). Here it is assumed that the body forces are absent.

$$\left.\begin{aligned} \frac{\partial \sigma_r}{\partial r} + \frac{\sigma_r + \sigma_\theta}{r} + \frac{1}{r}\frac{\partial \tau}{\partial \theta} &= 0 \\ \frac{\partial \tau}{\partial r} + \frac{2\tau}{r} + \frac{1}{r}\cdot\frac{\partial \sigma_\theta}{\partial \theta} &= 0 \end{aligned}\right\} \quad \text{——— 1a}$$

From these equations, the relation between the stress and strain follows as given below:

$$\left.\begin{aligned} \sigma_r &= \frac{E}{1-\mu^2}(\varepsilon_r + \mu\varepsilon_\theta) \\ \sigma_\theta &= \frac{E}{1-\mu^2}(\varepsilon_\theta + \mu\varepsilon_r) \\ \tau &= \frac{E}{2(1+\mu)}\gamma \end{aligned}\right\} \quad \text{——— 1b}$$

Finally, the relation between strain and displacement is given by the following equations:

$$\left.\begin{aligned} \varepsilon_r &= \frac{\partial u}{\partial r} \\ \varepsilon_\theta &= \frac{1}{r}\left(\frac{\partial v}{\partial \theta} + u\right) \\ \gamma &= \frac{\partial v}{\partial r} + \frac{1}{r}\left(\frac{\partial u}{\partial \theta} - v\right) \end{aligned}\right\} \quad \text{---------- 1c}$$

One knows that these equations hold good for even so called quasé plane, if one takes γ, τ, and u and v as the average quantities, the average being taken over the thickness of the body concerned.

Now, under the assumptions of the boundary conditions, (which will be given later) these equations are to be integrated.

The Method of Integration:

Since we know that the displacements are monovalent periodic functions of the angle θ, we develop the values of u and v in the following trigonometric series:

$$\begin{aligned} u &= \Sigma U_n \cos n\theta \\ v &= \Sigma V_n \sin n\theta \end{aligned} \qquad \ldots\ldots 2.$$

Where V_n and U_n are functions of the radial coordinates r, which will be determined later on.

So now, if we substitute the equation 2 in equations 1 b and 1 c, we get the following expression for the stresses

$$\left.\begin{aligned}
\gamma_r &= \frac{E}{1-\mu^2} \sum \cos(n\theta)\left[u'_n + u r^{-1}(u_n + n V_n)\right] \\
\gamma_\theta &= \frac{E}{1-\mu^2} \sum \cos(n\theta)\left[\mu u'_n + r^{-1}(u_n + n V_n)\right] \\
\gamma &= \frac{E}{2(1+\mu)} \sum \sin(n\theta)\left[V'_n - r^{-1}(n u_n + V_n)\right]
\end{aligned}\right\} 3$$

Where primes represent the differentiation with respect to r,

Introducing this equation 3 into the equation of equilibrium conditions, i.e., 1a, which gives the following total differential equation which will help determine U_n and V_n.

$$\left.\begin{aligned}
&u'' + u r^{-1} - u r^{-2}\left(1 + n^2 \frac{1-\mu}{2}\right) \\
&\quad + V' r^{-1} n \frac{1+\mu}{2} - V r^{-2} n \frac{3-\mu}{2} = 0 \\
&-u' r^{-1} n \frac{1+\mu}{2} - u r^{-2} n \frac{3-\mu}{2} + V'' \frac{1-\mu}{2} \\
&\quad + V' r^{-1} \frac{1-\mu}{2} - V r^{-2}\left(n^2 + \frac{1-\mu}{2}\right) = 0
\end{aligned}\right\} \text{---- } 4$$

The index n has been omitted in these equations for the present and they are of equal dimensionality so they can be integrated by the simple power of r and so we get

the following series.

$$u = \Sigma \alpha_i r^{\rho_i} \quad ; \quad V = \Sigma \beta_i r^{\rho_i}$$

Now this gives a very simple algebraic equation for the value of each ρ, when ρ is introduced in the equation 4. The roots of each of these equations are

$$\rho_i = \pm (1 \pm n) \qquad \text{——————————} \quad 5$$

Also

$$\rho_1 = 1+n \quad ; \quad \rho_2 = -(1+n)$$

$$\rho_3 = +(1-n) \quad ; \quad \rho_4 = -(1-n)$$

While between the constants α_i and β_i, the following relations hold good.

$$\beta_1 = -\alpha_1 \frac{n+q}{n-s} \quad ; \quad \beta_2 = \alpha_2$$

$$\beta_3 = \alpha_3 \frac{n-q}{n+s} \quad ; \quad \beta_4 = \alpha_4$$

Where q and S are the abbreviated forms, the value of which is given below.

$$q = \frac{4}{1+\mu} \quad ; \quad s = 2\frac{1-\mu}{1+\mu}$$

For $n = 0$ and $n = 1$, the case is especially simple. If we substitute $n = 0$ in equation 4 it gives two equations

for U_o and V_o and $n = 1$ yields a two-fold root $p_o = \pm 0$. Hence we get the following particular integral of logarithmic type:

$$n = 0$$

$$\left.\begin{aligned} u_o &= \alpha_1 r + \alpha_2 r^{-1} \\ V_o &= \beta_3 r + \beta_4 r^{-1} \end{aligned}\right\} \qquad \text{---------- 6a}$$

Here, the coefficient α gives a state of pure normal stress with purely radial displacement while coefficient β gives purely tangential stress with purely tangential displacement.

$$n = 1$$

$$\left.\begin{aligned} u_1 &= \alpha_1 r^2 + \alpha_2 r^{-2} + \alpha_3 + \alpha_4 \operatorname{Log} \frac{r}{r_i} \\ V_1 &= \alpha_1 r^2 \frac{5+\mu}{1-3\mu} + \alpha_2 r^{-2} - \alpha_2 - \alpha_4 \operatorname{Log} \frac{r}{r_i} \end{aligned}\right\} \qquad \text{---------- 6b}$$

$$n > 1$$

$$\left.\begin{aligned} u_n &= \alpha_1 r^{n+1} + \alpha_2 r^{-n-1} + \alpha_3 r^{n+1} + \alpha_4 r^{n-1} \\ V_n &= -\alpha_1 r^{n+1} \frac{n+q}{n-s} + \alpha_2 r^{-n-1} + \alpha_3 r^{-n+1} \frac{n-q}{n+s} - \alpha_4 r^{n-1} \end{aligned}\right\} \qquad \text{---- 6c}$$

From these equations, the displacements U and V are obtained immediately by the help of equation 2.

In order to derive the stresses from the equation 3, it is now necessary to introduce some abbreviations and different constants, in the above theory. For this purpose a new constant δ will be introduced in place of α and a certain reduced dimensionless stresses γ' and τ' in place of the original stresses γ and τ.

Further, the dimensionless coordinates and their reciprocals, which are in terms of external and internal radii, will also be used. These reciprocals are always < 1 due to their definition, and so, the equation 2 reduces to a convergent series, which is quite apparent.

The above mentioned reduced stresses will be as follows:

$$\gamma_r' = \gamma_r \frac{\pi^2}{8} \frac{r_a \delta}{P} \quad ; \quad \gamma_\theta' = \gamma_\theta \frac{\pi^2 r_a \delta}{8 P}$$

and

$$\tau = \tau \frac{\pi^2}{8} \times \frac{r_a \delta}{P} \qquad \text{7a}$$

Where P stands for the total force on the circumference of the circle. δ is the thickness of the eye and γ' γ_θ' and are the assumed new values.

The reduced radial coordinates and their reciprocals will be as follows.

$$\frac{r}{r_a} = \rho_a \quad ; \quad \frac{r_i}{r} = \rho_i \; ; \quad \frac{r_i}{r_a} = \eta \; ; \quad \frac{r_a}{r_i} = \frac{1}{\eta} = \lambda \qquad \text{7b}$$

To derive the coefficient we get the following equations:

When $n = 0$

$$\delta_1 = \alpha_1 \frac{E}{1-\mu} \frac{\pi^2}{8} \times \frac{R_a \delta}{P} \quad ; \quad \delta_2 = \alpha_2 \frac{E}{1+\mu} \times \frac{\pi^2 R_a \delta}{8 P R_i^2}$$

$$\delta_4 = \beta_4 \frac{E}{1+\mu} \times \frac{\pi^2 R_a \delta}{8 P R_i^2} \qquad \text{---------- 7c}$$

When $n = 1$

$$\delta_1 = \alpha_1 \frac{6E}{1-3\mu} \frac{\pi^2}{8} \frac{R_a^2 \delta}{P} \quad ; \quad \delta_2 = \alpha_2 \frac{2E}{1+\mu} \frac{\pi^2}{8} \frac{R_a \delta}{P R_i}$$

$$\delta_4 = \alpha_4 \frac{E\mu}{1-\mu^2} \frac{\pi^2}{8} \frac{R_a \delta}{P R_i} \qquad \text{---------- 7d}$$

For $n > 1$

$$\left.\begin{aligned}
\delta_1 &= \alpha_1 R_a^n \frac{E}{1+\mu} \frac{\pi^2}{8} \frac{R_a \delta}{P} \frac{(n+1)(n-2)}{n-2\frac{1-\mu}{1+\mu}} \\
\delta_2 &= \alpha_2 R_i - (n+2) \frac{E}{1+\mu} \frac{\pi^2}{8} \frac{R_a \delta}{P} (n+1) \\
\delta_3 &= \alpha_3 R_i^{-n} \frac{E}{1+\mu} \frac{\pi^2}{8} \frac{R_a \delta}{P} \frac{(n-1)(n+2)}{n+2\frac{1-\mu}{1+\mu}} \\
\delta_4 &= \alpha_4 R_a^{n-2} \frac{E}{1+\mu} \frac{\pi^2}{8} \frac{R_a \delta}{P} (1-n)
\end{aligned}\right\} \qquad \text{---------- 7e}$$

The magnitude $\frac{P}{r_a \delta}$ which appears in all the above equations is intimately tied up with the mean stress σ.

$$\sigma_m = \frac{P}{2(r_a - r_i)\delta} = \frac{P}{r_a \delta} \times \frac{1}{2(1-\eta)}$$

Or also with the mean pressure on the inside surface of the ring. So one can define the reduced stresses by the following expressions:

$$\sigma_r' = \frac{\sigma_r}{\sigma_r} \frac{\pi^2}{16\eta} \quad ; \sigma_\theta = \frac{\sigma_\theta}{\sigma_r} \frac{\pi^2}{16\eta}$$

$$\tau = \frac{\tau}{\sigma_r} \frac{\pi^2}{16\eta} \qquad \text{---------- 7a}$$

Where η = the ratio of the internal and external radii, or $\frac{r_i}{r_a}$

Now with these reduced coordinates of y_i and y_a and with the help of the new constants in δ_s, the reduced stresses σ' and τ' can be obtained as follows:

For $\eta = 0$

$$\left.\begin{aligned} \sigma_r' &= \delta_1 - \delta_2 y_i^2 \\ \sigma_\theta' &= \delta_1 + \delta_2 y_i^2 \\ \tau &= -\delta_4 y_i^2 \end{aligned}\right\} \qquad \text{---------- 8a}$$

For $n = 1$

$$\left.\begin{aligned} \nabla_R &= \cos\theta\left[\frac{\delta_1}{3} y_a - \delta_2 y_i^3 + \delta_4 y_i \frac{1}{\mu}\right] \\ \nabla'_\theta &= \cos\theta\left[\delta_1 y_a + \delta_2 y_i^3 + \delta_4 y_i\right] \\ \tau' &= \sin\theta\left[\frac{\delta_1}{3} y_a - \delta_2 y_i^3 - \delta_4 \frac{1-\mu}{2\mu} y_i\right] \end{aligned}\right\} \quad \delta_b$$

For $n > 1$

$$\left.\begin{aligned} \nabla'_R &= \cos n\theta\left[\delta_1 y_a^n - \delta_2 y_i^{n+2} + \delta_3 y_i^n - \delta_4 y_i^{n-2}\right] \\ \nabla'_\theta &= \cos n\theta\left[-\delta_1 y_a^n \frac{n+2}{n-1} + \delta_2 y_i^{n+2} - \delta_3 y_i^n \frac{n-2}{n+2} + \delta_4 y_a^{n-2}\right] \\ \tau &= \sin n\theta\left[-\delta_1 y_a^n \frac{n}{n-2} - \delta_2 y_i^{n+2} + \delta_3 y_i^n \frac{n}{n+2} + \delta_4 y_a^{n-2}\right] \end{aligned}\right\} \quad \delta_c$$

The Problem of the Eye-Ring:

The above is given a general theory. Coming to the application of that theory to the problem of the eye-ring, it is quite possible that we can assume the several

kinds of boundary conditions, the latter being dependent on the construction of the eye bar and on the manner of loading.

If one wishes to determine the distribution of stresses on the inside or outside surface of the eye and γ and τ then one has to develop the series shown in 6(a,b,c) and 8(a,b,c)

In our problem, we assume that the boundary conditions are as shown in the Fig. Ma i.e, at the inner surface.

(When $r = r_i$; $y_i = 1$ and $y_a = \frac{r_i}{r_a} = \eta$)

$\tau = 0$ from $\theta = 0$ to 2π

$\sigma_{ri} = 0$ from $\theta = \frac{\pi}{2}$ to $\frac{3\pi}{2}$

and

$\sigma_{ri} = -\frac{2P}{\pi r_i s} \cos\theta$ from $\theta = -\frac{\pi}{2}$ to $+\frac{\pi}{2}$

Similarly, for the outside surface:

(i.e. when $r = r_a$; $y_a = 1$; $y_i = \frac{r_i}{r_a} = \eta$)

$\tau = 0$ from $\theta = 0$ to 2π

$\sigma_{ra} = 0$ from $\theta = -\frac{\pi}{2}$ to $+\frac{\pi}{2}$

And

$\sigma_{ra} = -\frac{2P}{\pi r_a s} \cos\theta$ from $\theta = \frac{\pi}{2}$ to $\frac{3\pi}{2}$

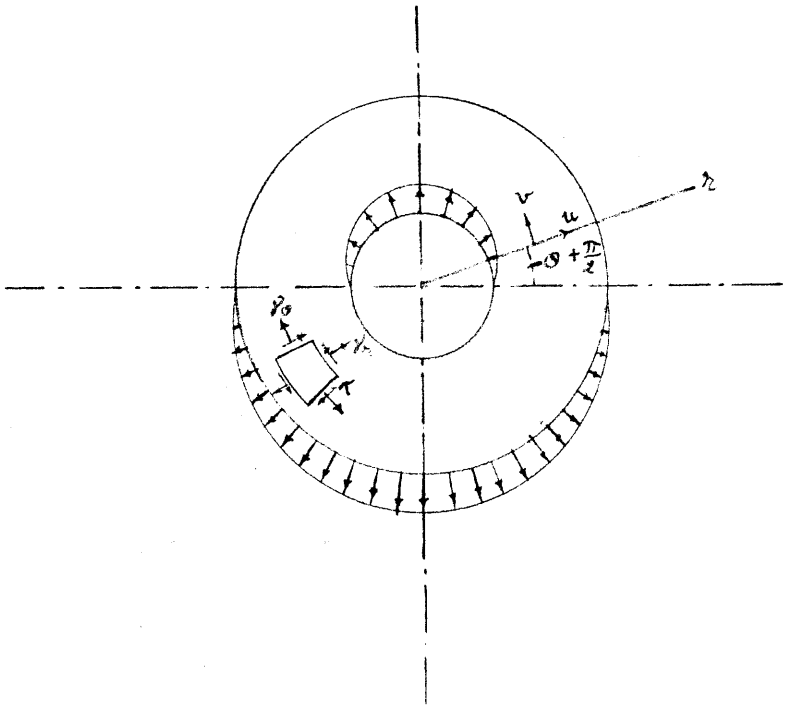
r
v
u
$\theta + \frac{\pi}{2}$
γ_θ
γ_r

Fig. Ma

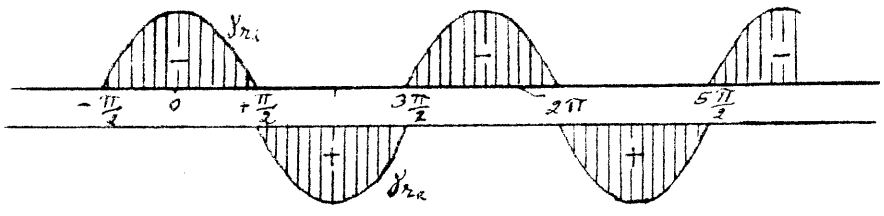
γ_{rr}
$-\frac{\pi}{2}$
0
$+\frac{\pi}{2}$
$\frac{3\pi}{2}$
2π
$\frac{5\pi}{2}$
$\gamma_{r\theta}$

Fig. Mb

Fig. M_b represents this surface condition in a graph form where, the angle θ is plotted on a straight line. This distribution, fulfills the requirements that the resulting force in the direction of the radius, for which $\theta = 0$ or π, is = P, at both inner and outer surface of the ring.

Now we have to develop the stresses σ_{ri} and σ_{ra} each in a trigonometric series, in such a way that they correspond to the above mentioned boundary conditions.

According to the well-known Fourier's method of determining the coefficient by means of definite integrals, one obtains the equation given below in 12, where only even values of n exist.

$$\sigma_{ri} = \tfrac{1}{2}C_{oi} + C_{1i}\cos\theta + C_{2i}\cos 2\theta + \cdots\cdots + C_{ni}\cos n\theta$$
$$\sigma_{ra} = -\tfrac{1}{2}C_{oa} + C_{1a}\cos\theta - C_{2a}\cos 2\theta - \cdots\cdots - C_{na}\cos n\theta$$

WHERE :—

$$C_{oi} = -\frac{4P}{\pi^2 r_i \delta} \quad ; \quad C_{oa} = -\frac{4P}{\pi^2 r_a \delta}$$

$$C_{1i} = -\frac{4P}{\pi^2 r_i \delta} \quad ; \quad C_{1a} = -\frac{P}{\pi^2 r_a \delta}$$

$$C_{ni} = (-1)^{n/2}\frac{4P}{\pi^2(n^2-1)r_i\delta}$$

$$C_{na} = (-1)^{n/2}\frac{4P}{\pi^2(n^2-1)r_a\delta}$$

——— 12

Now, if one determines the coefficient δ, he has to satisfy, besides the above mentioned conditions for the normal stresses at the outside, inside surfaces, also the condition that the τ, the shearing stress in zero. So this condition also should satisfy that equation.

Now, for mathematical simplification, if one introduces λ in place of η (which is its reciprocal) and after the comparison of the coefficient δ of the equations 8 (a,b,c) at the location of $r = r_i$ and $r = r_a$, with the coefficients c_{n_i} and c_{n_a} of the equation 12, he gets the following relations

When $n = 0$

$$-\frac{1}{H}\lambda = \delta_1 - \delta_2$$

$$+\frac{1}{H}\lambda^2 = \delta_1\lambda^2 - \delta_2$$

from which we get

$$\left.\begin{aligned}\delta_1 &= \frac{\lambda}{H(\lambda-1)}\\ \delta_2 &= \frac{\lambda^2}{H(\lambda-1)}\end{aligned}\right\} \qquad 13a$$

When $n = 1$

$$-\frac{\pi}{8}\lambda = \frac{\delta_1}{3\lambda} - \delta_2 + \delta_4\frac{1}{\mu}$$

$$-\frac{\pi}{8} = \frac{\delta_1}{3} - \delta_2\frac{1}{\lambda^3} + \delta_4\frac{1}{\mu\lambda}$$

$$0 = \frac{\delta_1}{3\lambda} - \delta_2 - \delta_4\frac{1-\mu}{2\mu}$$

$$0 = \frac{\delta_1}{3} - \frac{\delta_2}{\lambda^3} - \delta_4\frac{1-\mu}{2\mu\lambda}$$

For which we get

$$\delta_1 = -\frac{3\pi}{8}\,\frac{1-\mu}{3-\mu}\,\frac{\lambda^2}{\lambda^2+1}$$

$$\delta_2 = +\frac{\pi}{4}\,\frac{1-\mu}{3-\mu}\,\frac{\lambda^3}{\lambda^2+1}$$

$$\delta_4 = -\frac{\pi}{4}\,\frac{\mu}{3-\mu}\,\lambda$$

Here one of the equations is derived from the other because of the fact that the resultant force at both inside and outside the boundaries, must be equal, because, the rod is in equilibrium condition.

Now when $n > 1$

$$(-1)^{n/2}\frac{\lambda}{2(n^2-1)} = \delta_1\frac{1}{\lambda^n} - \delta_2 + \delta_3 - \delta_4\frac{1}{\lambda^{n-2}}$$

$$(-1)^{n/2}\frac{1}{2(n^2-1)} = -\delta_1 + \delta_2\frac{1}{\lambda^{n+2}} - \delta_3\frac{1}{\lambda^n} + \delta_4$$

AGAIN:—

$$0 = -\delta_1\frac{n}{1(n-2)}\cdot\frac{1}{\lambda^n} - \delta_2 + \delta_3\frac{n}{n+2} + \delta_4\frac{1}{\lambda^{n-2}}$$

$$0 = -\delta_1\frac{n}{n-2} - \delta_2\frac{1}{\lambda^{n+2}} + \delta_3\frac{n}{n+2}\frac{1}{\lambda^n} + \delta_4$$

And from that we get the equations

$$\left.\begin{aligned}\delta_1 &= (-1)^{n/2}\frac{(n-2)\left[\lambda^{n+1}(\lambda^{n+1}+1)(\lambda^{2n-2}-1)+(n+1)(\lambda^2-1)\lambda^{2n}(\lambda^{n-1}+1)\right]}{4(n^2-1)\left[(\lambda^{2n+2}-1)(\lambda^{2n-2}-1)(n^2-1)(\lambda^2-1)^2\lambda^{2n-2}\right]}\\[2ex]\delta_3 &= (-1)^{n/2}\frac{n+2}{4(n^2-1)}\,\frac{\lambda^n(\lambda^{2n-1}+1)(\lambda^{2n+2}-1)+(n-1)(\lambda^2-1)\lambda^{2n-1}(\lambda^{n+1}+1)}{(\lambda^{2n+2}-1)(\lambda^{2n-2}-1)-(n^2-1)(\lambda^2-1)^2\lambda^{2n-2}}\end{aligned}\right\}\ 13C$$

$$\left.\begin{aligned} \delta_2 &= (-1)^{n/2} \frac{-\lambda}{4(n^2-1)} - \delta_1 \frac{1}{(n-2)\lambda^n} + \delta_3 \frac{n+1}{n+2} \\ \delta_4 &= (-1)^{n/2} \frac{1}{4(n^2-1)} + \delta_1 \frac{n-1}{n-2} \\ &\quad + \delta_3 \frac{1}{(n+2)\lambda^n} \end{aligned}\right\} \quad 13c$$

Now, before we evaluate the above mentioned coefficients, let us put down the resulting general expression for the most important stress, i.e., the ring stress γ_θ, which is obtained from the equations 8 (a,b,c)

$$\left.\begin{aligned} \gamma'_\theta = \gamma_\theta \frac{\pi^2 \ell_a \delta}{8P} &= \delta_1^0 + \delta_2^0 y_i^2 + \cos\theta \left[\delta_1' y_i + \delta_2' y_i^3 + \delta_4' y_i\right] \\ &+ \sum_{n=2,4,6\ldots}^{\infty} \cos n\theta \left[y_a^n \left(-\delta_1^n \frac{n+2}{n-2} + \delta_4^n y_a^{-2}\right) \right. \\ &\left. + y_i^n \left(-\delta_3^{(n)} \frac{n-2}{n+2} + \delta_2^{(n)} y_i^2\right) \right] \end{aligned}\right\} \quad 14$$

Now we are merely interested in the sections where $\theta = 0$ or $\cos n\theta = 1$, i.e., on the straight vertical line of the resultant force P, and either the head or tail of the eye.

and also where $\theta = \pm \frac{\pi}{2}$ i.e., at the flanks of the eye.

Again in these sections too, only three points on the cross-sections may be taken to find out the stress curve for the section. So the following theory follows:

From the equation 14 we get:

When $\theta = 0$

$$\left.\begin{aligned} \sigma_\theta' = {} & \delta_1^\circ + \delta_2^\circ y_i^2 + \delta_1' y_a + \delta_2' y_i^3 + \delta_4' y_i \\ & + \sum \left[y_a^n \left(-\delta^{(n)} \frac{n+2}{n-2} + \delta_4^{(n)} y_a^{-2} \right) \right. \\ & \left. + y_i^{(n)} \left(-\delta_3^{(n)} \frac{n-2}{n+2} + \delta_2^{(n)} y_i^2 \right) \right] \end{aligned} \right\} \quad \text{— 15}$$

Now for the inner edge, i.e., when $y_a = \eta$ and $y_i = 1$ we get the equation

$$\left.\begin{aligned} \sigma_\theta = {} & \delta_1^\circ + \delta_2^\circ + \delta_1' \eta + \delta_2' + \delta_4' + \Sigma \left[\eta^n \left(-\delta_1^{(n)} \frac{n+2}{n-1} + \delta_4^{(n)} \eta^{-2} \right. \right. \\ & \left. \left. - \delta_3 \frac{n-2}{n+2} + \delta_2^{(n)} \right) \right] \end{aligned} \right\} \quad \text{— 15a}$$

Similarly, for the outside edge

i.e., when $y_a = 1$ and $y_i = \eta$

$$\left.\begin{aligned} \sigma_\theta' = {} & \delta_1^\circ + \delta_2^\circ \eta^2 + \delta_1' + \delta_2' \eta^3 + \delta_4' \eta + \Sigma \left[-\delta_1^{(n)} \frac{n+2}{n-2} + \delta_4^{(n)} \right. \\ & \left. + \eta^n \left(-\delta_3^{(n)} \frac{n-2}{n+2} + \delta_2 \eta^2 \right) \right] \end{aligned} \right\} \quad \text{— 15b}$$

For the point which is halfway between the inner and outer edges the equation will be as follows:

(i.e., when $y_i = \frac{2\eta}{1+\eta}$ and $y_a = \frac{1+\eta}{2}$)

$$\sigma'_\theta = \delta_1^0 + \delta_2^0 \frac{4\eta^2}{2(1+\eta^2)} + \delta_1' \frac{1+\eta}{2} + \delta_2 \frac{8\eta^3}{(1+\eta)^3} + \delta_4' \frac{2\eta}{1+\eta}$$

$$+ \sum \left[\frac{(1+\eta)^n}{2^n} \left\{ -\delta_1^{(n)} \frac{n+2}{n-2} + \delta_4^{(n)} \left(\frac{1+\eta}{2}\right)^{-2} \right.\right.$$

$$\left.\left. + \left(\frac{2\eta}{1+\eta}\right)^n \left(-\delta_3^{(n)} \frac{n-2}{n+2} + \delta_2^{(n)} \frac{4\eta^2}{(1+\eta)^2} \right) \right] \quad \text{——— 15c}$$

So from these three equations (15, a.b.c.) the stress curve for this section can be calculated. (The method of finding the constants in these equations will be given at a later stage).

Now for the section which is horizontal and passes through the center of the ring (AA in fig. 1), we get the following equations

Here $\theta = \frac{\pi}{2}$ $\quad (n = 2, 4, 6 \ldots\ldots\ldots)$

$\therefore \cos\theta = 0$ and $\cos n\theta = \cos \frac{2\pi}{2} = \pm 1 = (-1)^{n/2}$

So for this section we get the relation

$$(-1)^{n/2} \delta^{(n)} = \overline{\delta}(n)$$

So for this section we must multiply the constants obtained from the equation 13 (c), by the term $(-1)^{\frac{n}{2}}$ and

this way we must get δ s for each 'n'.

So now the equations for this section are as follows:-

$$\gamma'_\theta = \delta_1^\circ + \delta_2^\circ y_i^2 + \Sigma \left(-\bar{\delta}_1^{(n)} \frac{n+2}{n-2} y_a^n + \delta_4^{-(n)} y_a^{n-2} - \bar{\delta}_3^{(n)} \frac{n-2}{n+2} y_i^n + \bar{\delta}_2^{(n)} y_i^{n+2}\right) \quad \text{——— 16}$$

Applying this equation to the points at which we want to find the stress, we get the following equations. The point on the inner surface:-

$$\gamma'_\theta = \delta_1^\circ + \delta_2^\circ + \Sigma \left(-\bar{\delta}^{(n)} \frac{n+2}{n-2} \eta^n + \bar{\delta}_4^{(n)} \eta^{(n-2)} - \bar{\delta}_3^{(n)} \frac{n-2}{n+2} + \bar{\delta}_2^{(n)}\right) \quad \text{——— 16a}$$

For a point on the outside edge:-

$$\gamma'_\theta = \delta_1^\circ + \delta^\circ \eta^2 + \Sigma \left(-\bar{\delta}^{(n)} \frac{n+2}{n-2} + \bar{\delta}_3^{(n)} \frac{n-2}{n+2} \eta^n + \bar{\delta}_2^{(n)} \eta^{n+2}\right) \quad \text{——— 16b}$$

Similarly for the point at half way, the equation will be:-

$$\gamma'_\theta = \delta_1^\circ + \delta_2^\circ \frac{4\eta}{(1+\eta)^2} + \Sigma \left[-\bar{\delta}_1^{(n)} \frac{n+2}{n-2} \left(\frac{1+\eta}{2}\right)^n + \bar{\delta}_4^{(n)} \left(\frac{1+\eta}{2}\right)^{n-2} - \bar{\delta}_3^{(n)} \frac{n-2}{n+2} \left(\frac{2\eta}{1+\eta}\right)^n + \bar{\delta}_2^{(n)} \left(\frac{2\eta}{1+\eta}\right)^{n+2}\right] \quad \text{——— 16c}$$

Now, in all these six equations— 15 a b c and 16 a b c, the constants are found out from the following equations:-

$$\delta_1^0 + \delta_2^0 = \frac{\lambda(\lambda+1)}{4(\lambda-1)}$$

$$\delta_1^0 + \delta_2^0 \eta^2 = \frac{\lambda+1}{4(\lambda-1)}$$

$$\delta_1^1 + \delta_2^1 \frac{4\eta^2}{1+\eta^2} = \frac{\lambda(\lambda^2+1+6\lambda)}{4(\lambda-1)(\lambda+1)^2}$$

And also,

$$\delta_1^1 \eta + \delta_2^1 + \delta_4^1 = \frac{\pi}{8} \frac{\lambda[2\lambda^2(1-2\mu)-(3-\mu)]}{(3-\mu)(\lambda^2+1)}$$

$$\delta_1^1 + \delta_2^1 \eta^3 + \delta_4^1 \eta = \frac{\pi}{8} \frac{-\lambda^2(3-\mu)+2(1-2\mu)}{(3-\mu)(\lambda^2+1)}$$

Similarly,

$$\delta_1^1 \frac{1+\eta}{2} + \delta_2^1 \frac{8\eta^2}{(1+\eta)^3} + \delta_4^1 \frac{2\eta}{1+\eta}$$

$$= \frac{\pi}{8} \frac{[3\lambda(1-\mu)(\lambda+1)^4 + 16(1-\mu)\lambda^2 - 4\mu(\lambda+1)^2(\lambda^2+1)]\lambda}{(3-\mu)(\lambda^2+1)(\lambda+1)^3}$$

And $\delta_1^{(n)}$ $\delta_2^{(n)}$.....etc. means the corresponding values of δ_1 δ_2 δ_3 and δ_4 for each value of n.

So from these equations ~~xx xxx~~one can evaluate the value of stresses at any point on these crossections.

Here, it is interesting to note that, the ~~xxixxxxix~~ Poisson's ratio has the effect on the ~~xxxxixxx xxxxx~~ stress

curve
for the section where $\theta = 0$ i.e. where the pin has a contact with the main ring. This shows how it is essential to make the pin, of the same material as that of the main body.

The author has used the equations 16 a b c to determine the stress curve for the section AA (Fig. 1) The results of his calculations and the values of the constants are given on the next pages. The curve is shown in the Fig 25.

The author's ratios of $\frac{ra}{ri}$ being very small, the author had to work out the series upto fifteen places.

All the calculations were done on a calculating machine and ~~so~~ are very accurate.

The tables of the constants δ_1, δ_2 etc. can be used for the calculations for the stress curve for any other section, by this method.

———:———

Calculated Results

The values of the const. $\bar{\delta}^{(n)}$

n	$\bar{\delta}_1^{(n)}$	$\bar{\delta}_2^{(n)}$	$\bar{\delta}_3^{(n)}$	$\bar{\delta}_4^{(n)}$
2	4.378 (n-2)	12.01875000	19.30909000	7.05245000
4	.24666665	.67262000	.87706660	.42885000
6	.08891278	.19410000	.23690000	.12551700
8	.04618000	.08415900	.10023649	.05868400
10	.02992853	.05098700	.05963579	.03638900
12	.02208000	.03611110	.04156048	.02610900
14	.01757551	.02794020	.03172529	.02033340
16	.01489209	.02321470	.02602520	.01698200
18	.01299267	.01993700	.02211824	.01457910
20	.01160211	.01762370	.01932529	.01287980
22	.01051936	.01579240	.01722515	.01159877
24	.00965526	.01440680	.01557362	.01053634
26	.00893784	.01321390	.01423075	.00968220
28	.00832622	.01225400	.01311325	.00895987
30	.00779969	.01141900	.01216809	.00833803
		13.21252880		7.84188851

n	$\bar{\delta}_1^{(n)}\left(\frac{n+2}{n-2}\right)\eta^n$	$\bar{\delta}_4^{(n)}(\eta)^{n-2}$	$\bar{\delta}_3^{(n)}\frac{n-2}{n+2}$	$\bar{\delta}_1^{(n)}\frac{n+2}{n-2}$
2	9.40044160	7.05245000	.0[illegible]000000	17.51200000
4	.21319429	.23020668	.29235667	.74000100
6	.02749190	.03616145	.11845000	.17782600
8	.00639054	.00907255	.06000000	.07696666
10	.00201107	.00302138	.03976000	.04489500
12	.00073942	.00116368	.02968571	.03091200
14	.00030090	.00048637	.02379375	.02343466
16	.00013198	.00021805	.02024556	.01914686
18	.00006009	.00010049	.01769440	.01624000
20	.00002816	.00004766	.01581160	.01418036
22	.00001346	.00002304	.01435433	.01262328
24	.00000653	.00001124	.01317715	.01141081
26	.00000320	.00000554	.01219800	.01042767
28	.00000158	.00000275	.01136486	.00960692
30	.00000079	.00000137	.01064700	.00891394
	9.65081551	7.33297225	.67953903	18.70858516

n	$\bar{\delta}_3^{(n)}\left(\frac{n-2}{n+2}\right)\eta^n$	$\bar{\delta}_2^{(n)}(\eta)^{n+2}$	$\bar{\delta}_1^{(n)}\left(\frac{n+2}{n-2}\right)\left(\frac{1+\eta}{2}\right)^n$	$\bar{\delta}_4^{(n)}\left(\frac{1+\eta}{2}\right)^{n-2}$
2	.00000000	3.46260187	13.14450720	7.05245000
4	.08422805	.10398705	.41684763	.32189481
6	.01831237	.01611612	.07520262	.07070542
8	.00498180	.00375101	.02442933	.02481746
10	.00177210	.00121961	.01069399	.01154987
12	.00071009	.00046367	.00552707	.00621916
14	.00030551	.00019259	.00314494	.00363554
16	.00013955	.00008589	.00192810	.00227898
18	.00006547	.00003959	.00122791	.00146812
20	.00003140	.00001879	.00080474	.00097377
22	.00001530	.00000904	.00053775	.00065823
24	.00000754	.00000443	.00036492	.00044885
26	.00000375	.00000218	.00025037	.00030964
28	.00000187	.00000108	.00017302	.00021513
30	.00000094	.00000054	.00012052	.00015017
	.11057574	3.58849346	13.68576011	7.49777515

n	$\overline{\delta}_3^{(n)}\left(\frac{n-2}{n+2}\right)\left(\frac{2n}{1+n}\right)^n$	$\overline{\delta}_2^{(n)}\left(\frac{2n}{1+n}\right)^{n+2}$
2	.00000000	6.15843312
4	.14980373	.24664975
6	.04343562	.05095125
8	.01575000	.01581348
10	.00747090	.00685816
12	.00399331	.00347713
14	.00229112	.00192590
16	.00139556	.00114543
18	.00087302	.00070428
20	.00055848	.00044553
22	.00036287	.00028568
24	.00023837	.00018657
26	.00015796	.00012252
28	.00010538	.00008133
30	.00007066	.00005425
	.22650698	6.48713438

AGAIN,

$$\delta_1^\circ + \delta_2^\circ = \frac{\lambda(\lambda+1)}{4(\lambda-1)} = \frac{1.365 \times 2.365}{4 \times .365}$$

$$= 2.211$$

$$\delta_1^\circ + \delta_2^\circ \eta^2 = \frac{\lambda+1}{4(\lambda-1)} = \frac{2.365}{4 \times .365}$$

$$= 1.619$$

$$\delta_1^\circ + \delta_2^\circ \left(\frac{4\eta^2}{1+\eta^2}\right) = \frac{\lambda(\lambda^2+1+6\lambda)}{4(\lambda-1)(\lambda+1)^2}$$

$$= \frac{1.365 \times (1.863+1+8.190)}{4(.365)(2.365)^2}$$

$$= 1.847$$

Now applying the method for our case, Section AA, the calculations for the stresses will be as follows:—

The reduced stress at the inner edge:—

$$\nu_B' = \delta_1^\circ + \delta_2^\circ + \sum -\bar{\delta}_1^{(n)} \frac{n+2}{n-2} \eta^n + \bar{\delta}^{(n)} \eta^{n-2} - \bar{\delta}_3^{(n)} \frac{n-2}{n+2} + \bar{\delta}_2^{(n)}$$

$$= 2.211 - 9.6508 + 7.3330 - .6795 + 13.2125$$

$$= 12.4162$$

The reduced stress at the outside edge is calculated as below :-

$$\bar{\sigma}_\theta' = \bar{\sigma}_1^0 + \bar{\sigma}_2^0 \eta^2 + \sum \left(-\bar{\sigma}^{(n)} \frac{n+2}{n-2} + \bar{\sigma}_4^{(n)} - \bar{\sigma}_3^{(n)} \frac{n-2}{n+2} \eta^n + \bar{\sigma}_2^{(n)} \eta^{n+2} \right)$$

$$= 1.619 - 18.7086 + 7.8419 + .1106 + 3.5885$$

$$= -3.7698$$

Similarly, the reduced stress on the central point on the section AA will be calculated as follows :-

$$\bar{\sigma}_\theta' = \bar{\sigma}_1^0 + \bar{\sigma}_2^0 \frac{4\eta}{(1+\eta)^2} + \sum \left(-\bar{\sigma}_1^{(n)} \frac{n+2}{n-2} \left(\frac{1+\eta}{2} \right) + \bar{\sigma}_4^{(n)} \left(\frac{1+\eta}{2} \right)^{n-2} - \bar{\sigma}_3^{(n)} \frac{n-2}{n+2} \left(\frac{2\eta}{1+\eta} \right)^n + \bar{\sigma}_2^{(n)} \left(\frac{2\eta}{1+\eta} \right)^{n+2} \right)$$

$$= 1.847 - 13.6858 + 7.4978 - .2265 + 6.4871$$

$$= \frac{1.9196}{2}$$

Now

$$\sigma_\theta = \sigma'_\theta \times \frac{8P}{\pi^2 R_2 S} = \frac{8 \times 152.5}{\pi^2 \times .703 \times .744} \sigma'_\theta$$

$$= 236.3 \sigma'_\theta$$

So the stresses at the above three point will be as follows :—

Stress at the inner edge :— (Section A A)

$$\sigma_\theta = 236.3 \times 12.4262 = 2941 \text{ lbs/}_0.$$

Stress at the central point will be

$$\sigma_\theta = 236.3 \times 1.9196 = 453.8 \text{ lbs/}_0"$$

Stress at the outer edge will be :—

$$\sigma_\theta = -236.3 \times 5.7618 = -\frac{1365}{2} \text{ lbs/}_0"$$

Comparing these stresses with average stress we get

$$\frac{\partial \theta}{\partial \ell} = \frac{2940}{199} = \frac{14.8}{\ell}$$

For central point :-

$$\frac{\partial \theta}{\partial \ell} = \frac{453.8}{199} = \frac{2.28}{\ell}$$

For outside edge :-

$$\frac{\partial \theta}{\partial \ell} = \frac{-1365}{199} = \frac{-6.86}{\ell}$$

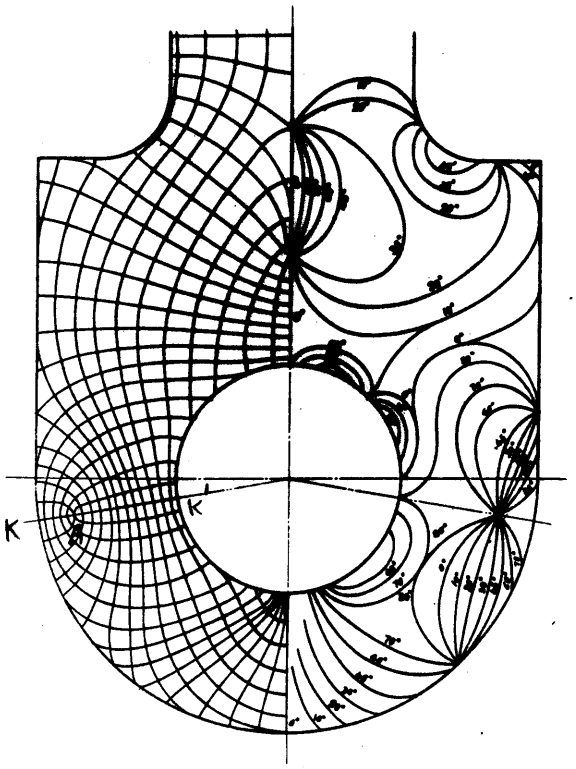

FIG 26

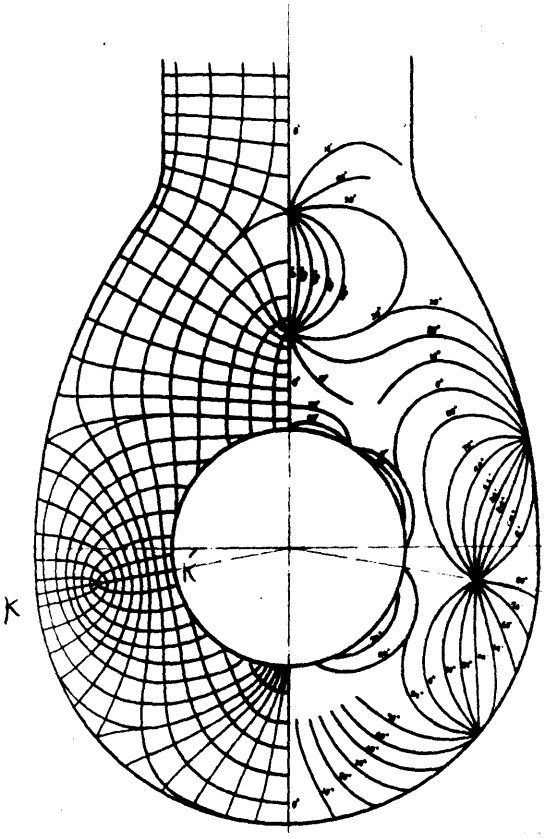

FIG. 27

Discussion of the Results:-

The main point that arises in this case is that the author's mathematical calculations do not tally a bit with those obtained from the experimental results. Naturally, the question arises about the correctness of the mathematical assumptions, because the author has taken great pains in checking the results of the interferometer readings and has not the slightest doubt about their correctness, and of course the fringe photograph is already there to prove the correctness of the p-q curves.

After a thorough study of the subject, and particularly after the study of the three articles - one by Mr. Takemura, the other by Mr. Reissner, and the third by Dr. Mathar -- the author of the present paper has come to the conclusion that, the assumptions made at the beginning of the mathematical calculations do not represent exactly the condition as is present in this case. Of course if the manner of fit is changed, then these assumptions may be applied in that case. The results obtained by the author in his mathematical work are given here in the hope that they may be of use to other investigators who may try the other corresponding fit.

To explain the above paragraph in detail, and to give the author's interpretation of the results of the present work, it is essential that the reader should have

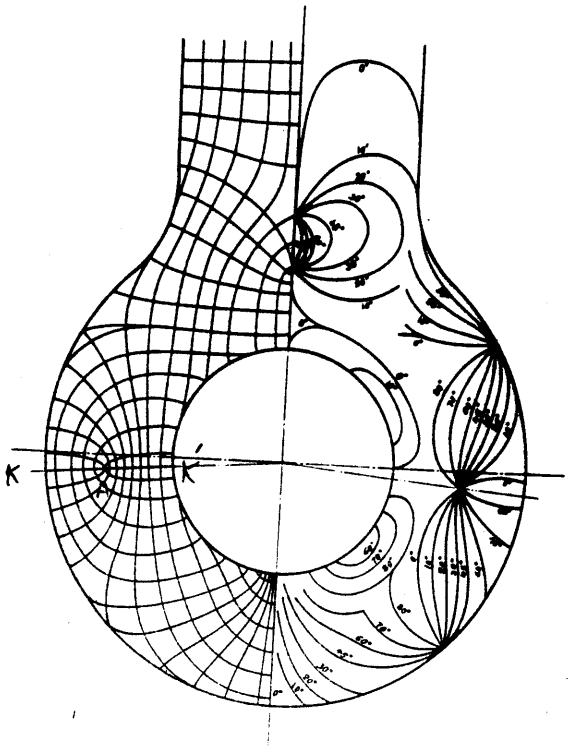

Fig. 38

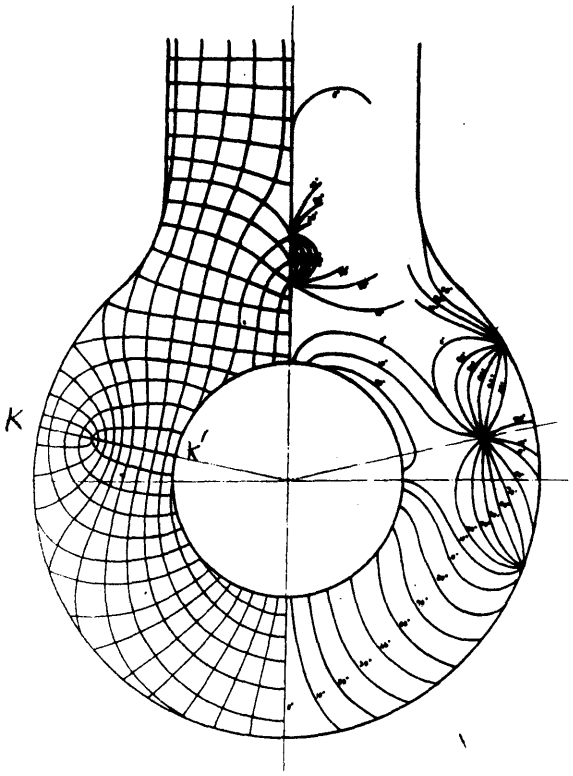

FIG. 27

a general idea of the problem of the connecting rod, and for that reason, the author would like to discuss the case in general and then would explain how the results obtained in this paper are in tune with that discussion. The discussion is based on the work of the above mentioned three scientists.

General Discussion;

The stress distribution and the position of the stress concentration in the eye section of a connecting rod depend on many different variables. For example, if we change the shape of the eye end, the stress distribution changes completely. In this respect, the author would like to give the results obtained by Mr. Takemura. The photographs in Fig. 26 to 29 show how the change in the shape of the eye ring changes the pattern of the isoclinics and the stress trajectories completely, so much so that the position of the singular point* (A in each photograph) also changes.

According to Mr. Takemura, "---- The lines of the principal stresses in the eye end are generally curved, but there is one line which may be taken as straight or very nearly so (KK' in our photographs).

"For the sake of simplicity, let it be called the "Principal Lines". The stress at the cross-section of these "Principal Lines" with the inner edge of the eye, was

* These photographs are reproduced from the article by Mr. Takemura and Yahei Hosokawa. The letters A and KK are introduced by the author.

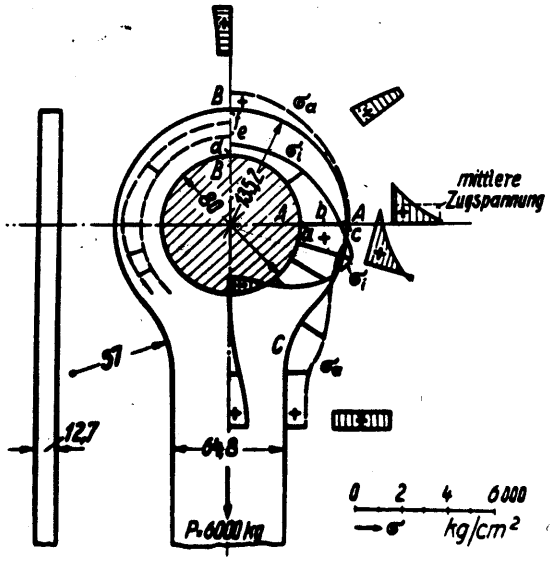

Abb. 1. Spannungserteilung in Stangenköpfen-Bolzen ohne Spiel.

FIG. 30

found to be maximum by means of "the Comparison Test Piece". Again, let this intersection be called the "Principal Point" (K' in our photographs).

"The position of this 'principal point' varies according to the shape of the contours of the eye shaped end.--"

The author of the present paper would like to call this "Principal Line" as "The Line of the Maximum Stress". So, according to the results obtained by Mr. Takemura, the positions of the "Line of Maximum Stress" changes with the shape of the eye end. (Photographs in Figs. 26 - 29).

The second main factor that affects the position of the Line of Maximum Stress is that of the clearance of the pin fitted inside the eye-hole. This is clearly seen from the comparison of the two photographs in Figs. 28 and 29. (In the first case the pin is loose while in the second the pin just fits the eye).

Again the same fact is proved from the results obtained by Dr. Mathar in 1928. As a matter of fact, in his article, Dr. Mathar gives in detail the effect of the clearances on the stresses. His results are all experimental ones. The author of the present paper has reproduced some of his figures on the next page. From these three photographs (Figs. 30 - 32) one sees that in case of a tight fit (Fig. 30) the stress across the section horizontal to the centre line of the connecting rod, and passing through the centre of the eye, does not become zero as it does on the

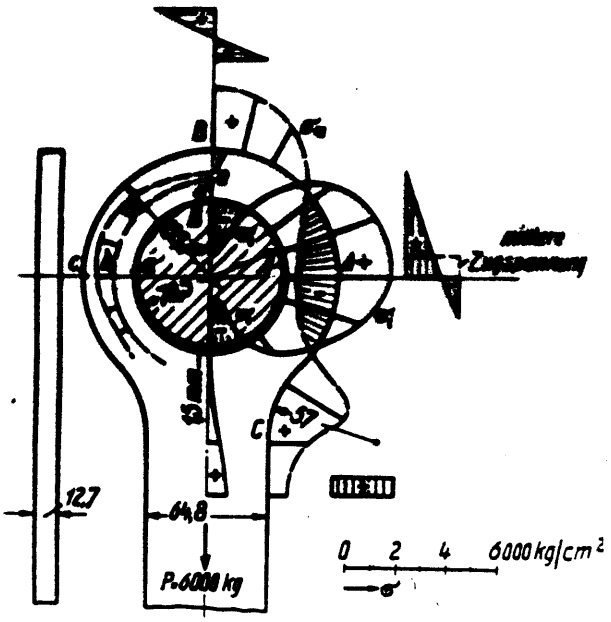

Abb. 2. Spannungsverteilung in Stangenköpfen-Bolzen mit 1,5 mm Spiel.

FIG. 31

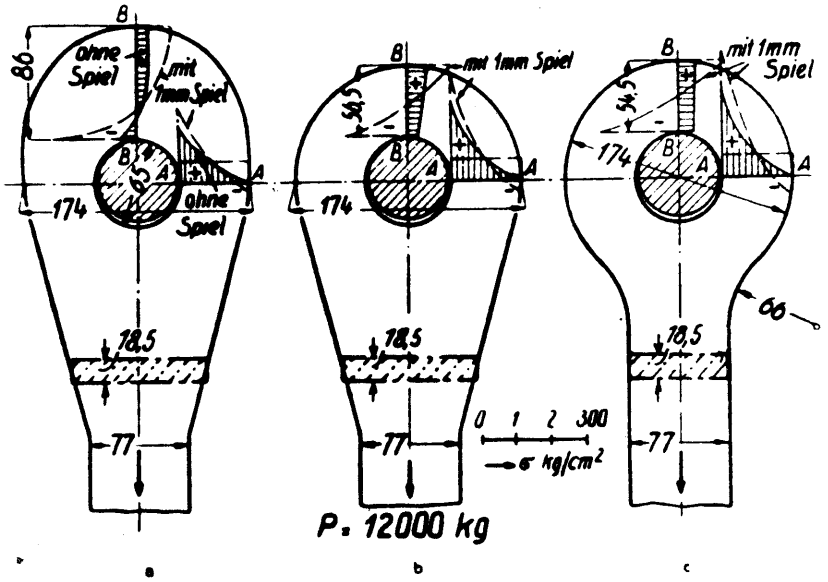

Abb. 4. Spannungen in Augenstäben.

FIG 32

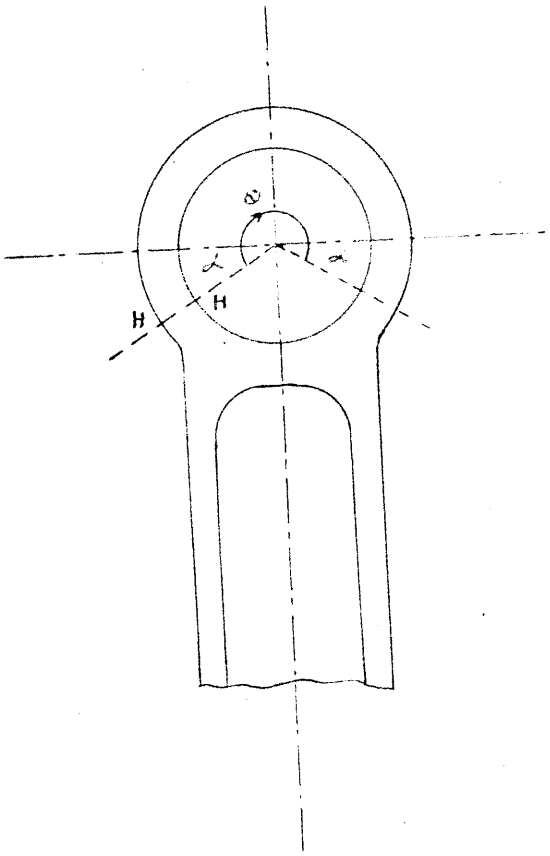

Fig. 33

same section in Fig. 31.

From this data the author of the present paper concludes that

a) The position of the Line of Maximum Stress depends on the shape of the eye end.

b) It also depends on the clearance of the pin.

c) It is quite possible (though the author has no conclusive proof for this statement) that this Line of Maximum Stress may be exactly situated at the point on the circle from which the loading contact begins. That is, say, the angle of contact is represented by the angle in Fig. 33, then the section HH (Fig. 33) would give the Line of Maximum Stress. The author would like to give the following proof in support of his statement.

In Fig. 30 obtained by experiments by Dr. Mathar, the Maximum Stress occurs not at the section AA but at the section ac. This is a case of "force fit" and it is quite sensible to believe that in this case, the angle of contact must be more than 180°, and possibly just ending at the section ac.

Again, in the case of Fig. 34 where Mr. H.Reissner has calculated the stresses mathematically, one observes that, the maximum stress concentration occurs at the top point of the inside edge. Now in this case Mr. Reissner has assumed that the load is applied at the topmost point, (i.e., the mathematical angle of contact is zero). The

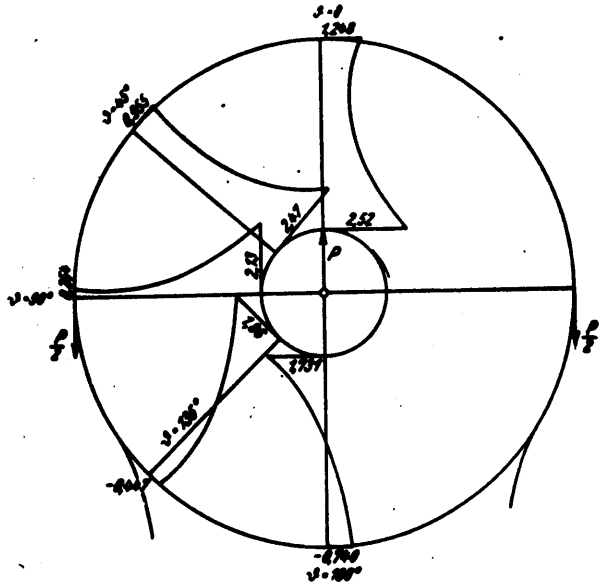

Abb. 5. Spannungsvertoilung $\frac{v_\vartheta}{v_m}$ zu Abb. 4.

FIG. 34

stress concentration in this case is maximum at this point of contact, and is less at any other point on any other section.

Again, if the reader studies the fringe photograph given in the present paper, he will see that the angle of contact in this case is also more than 180°. In his experiments the author has used a "tight fit" and so this case too supports the above statement.

All these facts tend to show that the above statement about the position of the "line of Maximum stress" must be true.

Comparison of ~~My~~ Experimental Results with Those of the Others

If the reader compares the curves obtained in this experiment with that obtained by Dr. Mathar in his experiment with an eye bar having a tight fit, (Fig. 30) he will observe that both the curves are similar, i.e., they go from maximum value at the inside edge to some positive value at the outside edge, and this positive value at the outside edge is also very small. In the results of this paper, the author gets similar results. The only difference that is observed is that, while Dr. Mathar gets a slight concave curve, the author of the present paper, gets a slightly convex curve.

If the reader promises not to charge the author with being too bold, the author would like to state that, as far as the trend of the curve is concerned, the results ob-

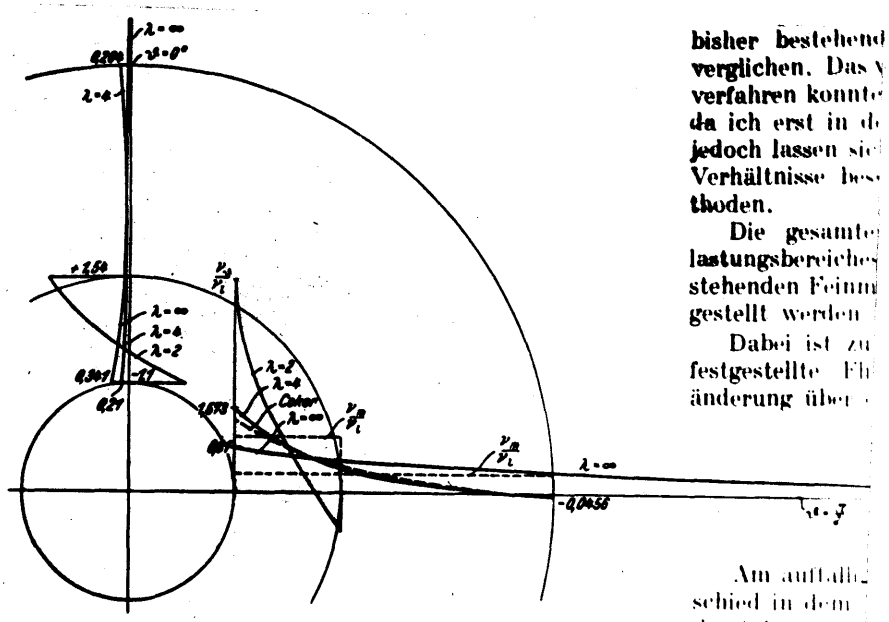

Abb 7. Spannungsdiagramme bei wechselnden Ringbreiten.

bisher bestehend
verglichen. Das
verfahren konnte
da ich erst in d
jedoch lassen sic
Verhältnisse bes
thoden.

Die gesamte
lastungsbereiches
stehenden Feinm
gestellt werden

Dabei ist zu
festgestellte Fl
änderung über

Am auffalli
schied in dem
des inhegende
des Auges b
strenrunne

FIG. 35

tained in this paper are more reliable; the reason being that, while Dr. Mathar must have drawn his curves from the results obtained just for the three points, the curve given in this paper, is drawn from many points.

Mathematical Work:-

Coming to the mathematical results obtained in his work, the author is sorry to state that, as the assumptions that he had made in his calculations did not agree with the stress condition that was present during his experimental test, his mathematical curve is quite different than that of the experimental work.

Of course the curve obtained from the mathematical calculations is exactly like what one would expect from these calculations. For example, if the reader compares this curve with those obtained by Mr. Reissner, he will see that the curve given in this paper is just as one would expect. (Fig. 35). Mr. Reissner has calculated the stresses at the section AA for a rod having the ratio of $\frac{r_a}{r_i} = \infty$, 4 and 2. The author of the present paper has calculated the same curve for the rod having that ratio = 1.365 (which was the ratio obtained from the actual connecting rod).

The author from his experience on this problem thinks that the stress condition that one should assume in Fig. 36 and not as assumed in these calculations, is for the case of a connecting rod having "force fit". Mr. Reissner

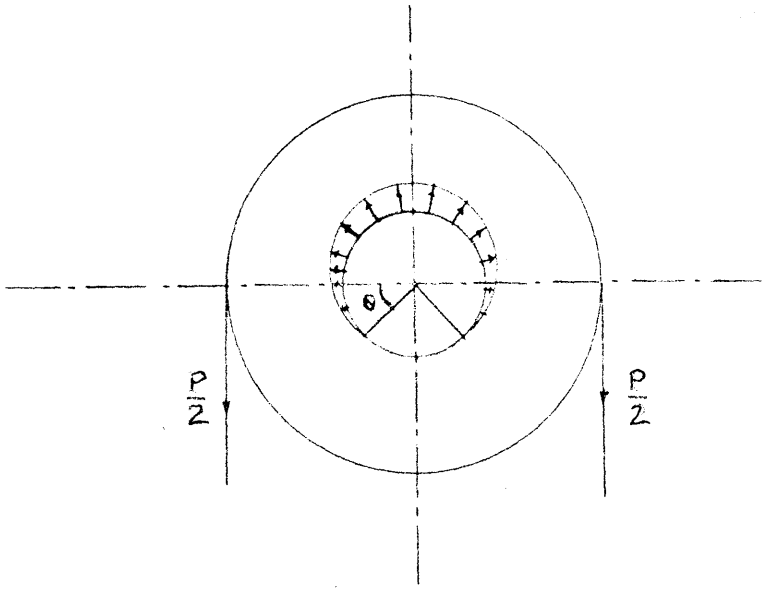

Fig. 36

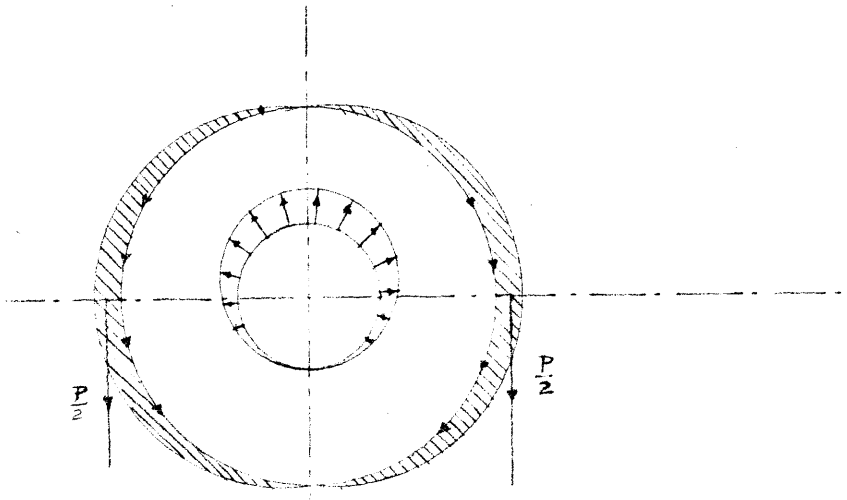

Boundry conditions :-

At inside edge $y_2 = y_1(1+\cos\theta)$, $\tau = 0$

At outside edge $y_1 = 0$, $\tau = \tau_1 \sin\theta$

Fig. 37

has also treated the problem considering the stress conditions as shown in Fig. 37. This case is nearer to the actual condition of a "force fit" though the existence of shear shown at the outside boundary is a debatable question. The curves in Fig. 35 are those obtained by Mr. Reissner from his mathematical work, the conditions being the same as those assumed in the mathematical work of this paper.

A Few Words to Future Investigators:-

To summarize the above discussion, the author would like to give a few suggestions to the future investigator in a nutshell form.

a) He should not bother about treating the subject by three dimensional method.

b) He should first decide the manner of loading i.e. whether he wants to keep a clearance or intends to have a "force fit". All the calculations depend on these conditions.

c) From the study of his fringe photograph, he should first figure out the actual angle of contact between the pin and the rod. This is very essential because the position of the Line of Maximum Stress depends on this angle, and also, this angle is to be used in the assumptions that one has to make in the mathematical calculations.

d) Having done this, he should select the section at the point where the contact between the inside edge of the eye bar and the pin just begins. (HH in Fig. 33) and then find

out the p+q and p-q curves for this section. This will give the maximum stress concentration in the rod.

e) Unlike the author of this paper, he should start his mathematical work only after finishing his experimental work completely, and after determining the boundary stress condition from his experiment. This would enable him to assume the same conditions at the edges that would be present in his problem at the time of loading.

f) If he takes the case of a tight fit, the stress conditions at the outside and inside edges would be something as shown in Fig. 36. A method of integration for such an angle of contact must be found out.

g) The different methods of attack given by Mr. Reissner in his article will be of very much help to the investigator. He must make it a point to study that article thoroughly.

The Suggestions to the Designer of a Connecting Rod

As the reader would agree, it is very hard to give the concrete suggestions to a designer, from the experience of the stress distribution of a single connecting rod. But, nevertheless, the author would jot down a few points which a designer might consider and study; and which might be of some use to him.

a) From the experimental results of Mr. Takemura and his colleague, and from the results and curves of the experiments performed by the author of the present paper, it is

quite clear that, the radii of the curvatures at the junction of the eye ring and the stem (I section) must be made as large as possible. The study of the p and q curves for the section BB (Fig. 21) show how the peak occurs very near the edge of this curve. Mr. Takemura suggests that the shape of the eye should be as shown in Fig. 27. (which is produced from his article). The author of the presentpaper endorses that statement.

b) If one studies the region shown by the dotted lines in Fig. 9 one sees that this region is not subjected to any appreciable stress, tension or compression, during the tension tests. So it is quite possible that the metal in this region may be reduced to a considerable extent. The author would like to go even so far as to suggest that if a hole is drilled in this region the stress concentration due to that hole will not be very appreciable because of the low value of the original stress. This will reduce the weight of the connecting rod. We may use this removed metal to fill in the curvature at the fillet. This will make the stress curve for BB (Fig. 21) almost uniform.

Besides the above advantage, the author of the present paper thinks that this drilling of the hole would also make the load on the bearing of the pin uniform, and so naturally would help the design of the bearing.

Of course all of the above suggestions are put forward only after the study of the stress conditions in the rod during

the tensile loading, and so the reader is advised to study the rod under compression before adopting the suggestions.

Even if one does not agree to drill a hole in the eye ring as suggested above, he may at least make the groove which forms the eye section of the stem, such that, it goes almost near the inner edge of the ring. This will not produce any appreciable change in the stress variation in the rod. (of course only under tension). This would reduce the metal and would permit the addition of metal near the fillet.

c) The author has not been able to reason out the curve for the cross-section of the stem (I section) Fig. 24. Here, unlike the expectation, the stress is not uniform, but instead, the stress curve droops down at the edges.

This may possibly be explained from the curve for the section BB (Fig. 21). This curve means that the transferance of the force from the eye ring to the stem may be taking place in the same manner as the p curve for this section. So, naturally, the stresses in the stem will not become uniform for a long distance. From the p curve for this section BB one sees that the stress at the edge of the eye is less than the peak point (which is .05" from the edge) of the curve. This may be the reason why the curve for the stem is drooping at the edges.

If the above argument is true then it follows that the width of the I section in this case is more than what is

required for the tension loading. Besides enlarging the radii of the fillets, the width of the stem may be reduced gradually with advantage.

d) Before adopting any of the above suggestions it is essential that the connecting rod be tested under compression. The studying of the rod under dynamic conditions would also enlighten the designers to a considerable extent.

e) The failure that takes place in actual connecting rods is always at the section HH (Fig. 33). The author thinks that this is solely due to the fatigue of the metal at this section. It is quite possible that, under compression, the section HH is subjected to a stress curve which is exactly opposite to the stress curve under tension. Due to this the actual range of the stress for this section would be greater than that of the section AA. This would affect the 'Natural Elastic Range" of the material. This problem of cyclic variation also brings in the factor of time, i.e., the connecting rods of the high speed engines would be much more liable to the fatigue failure of this kind than those of the slow speed engines.

f) The study of the mathematical treatment of Mr. Reissner, and the experimental work of Dr. Mathar show that the "force fit" would bring down the Line of Maximum Stress nearer to the section HH (Fig. 33) than to the section AA. (Fig. 1). This should be avoided for the reasons given above in (e). Naturally, the following deductions follow:

i) The bushing of the bearing metal fitted inside the eye ring should not be tight. A stopper to stop the revolving tendency would permit the bushing to be made of the "sliding type."

ii) In some engines, the pin is fitted tightly inside the connecting rod eye while the former is allowed to rock in the piston bushings. The above discussion in section (e) shows that this will bring the Line of Maximum Stress nearer to the section HH (Fig. 33) and so the practice should be discontinued.

———————:———————

BIBLIOGRAPHY

1. "Das Augenstabproblem und Verwandte Aufgaben" By H. Reisner "Jahrbuch" Der Wissenschaftlichen Oesellschaft 1928 p. 126- 137

2. Uber die Spannungsverteilung in Stangenkopfen" by I.J.Mathar Forschungsabbeiten Heft 306. 1928 p. 1 - 12

3. " Eye - shaped End of Bar Investigated by Photo-Elastic Method " by Kango Takemura and Yahei Hosokawa. Reports of the Aeronautical Research Institute, Tokyo Imperial University, Vol 11. 1928, p. 127 - 143

4. "Stress Analysis is Simplified by New Method" by K.E.Bisshopp Machine Design, Aug. 1937, p.40

5. " Computing Eye-Rod Stresses of a Connecting Rod" by K.E.Bisshopp. Machine Design, Sept. 1939, p. 47-48.

6. "Theory of Elasticity" by S. Timoshenko, p. 120

7. "Design of Small End of an Aero-Engine Connecting Rod". by Angle, Automotive Industries, March 9, 1935, p.349-51

8. "Entwicklung Von Triedwerksteihen" by Volk V.D.I.Ziet, Oct. 22, 1938, p 1233-9

9. "Theories Und Berechnung der Eisernen Bruechen" by Bleich p. 256.

XXXXXXXXXXXXXXX